

Logical Operators and Derived Automorphisms of Tile Codes

Nikolas P. Breuckmann¹ Shin Ho Choe^{2*} Jens Niklas Eberhardt³
 Francisco Revson Fernandes Pereira² Vincent Steffan^{2†}

¹Breuqmann Ltd., Redcross Village, BS2 0BB, Bristol, United Kingdom
²IQM Quantum Computers, Georg-Brauchle-Ring 23–25, 80992 Munich, Germany
³Institute of Mathematics, Johannes Gutenberg-Universität, Mainz, Germany

November 19, 2025

Abstract

The recently introduced tile codes are a promising alternative to surface codes, combining two-dimensional locality with higher encoding efficiency. While surface codes are well understood in terms of their logical operators and boundary behavior, much less is known about tile codes. In this work, we establish a natural and precise description of their logical operator space. We prove that, under mild assumptions, any tile code admits a canonical symplectic basis of logical operators supported along lattice boundaries, which can be generated efficiently by a simple cellular automaton with the number of update rules only depending on the non-locality of the tile code. Further, we develop algebraic and algebro-geometric frameworks for tile codes, by resolving them by translationally invariant Pauli stabilizer models and showing that they arise as derived sections of a Koszul complex on $\mathbb{P}^1 \times \mathbb{P}^1$. Finally, we introduce the concept of derived automorphisms for quantum codes. These are automorphism-like operations that can exist even for codes that do not have symmetries. We explain how derived automorphisms can be implemented for tile codes in a low-overhead and fault-tolerant manner by extending the lattice on one side and shrinking it on the other. While this operation is trivial for the surface code, it induces a product of logical CNOT gates on the encoded information. Our results provide new structural insights into tile codes and lay the groundwork for tile codes as building blocks for fault-tolerant quantum computation.

1 Introduction

It is widely accepted that quantum error correction is an indispensable ingredient for large-scale quantum computing. The currently leading proposal for implementing quantum error correction and fault-tolerance is the surface code [3, 12]. This is owed to its good error correction capabilities and easy-to-implement planar layout. However, recently, there have been several breakthroughs in the construction of quantum codes that are much more efficient and could lead to huge savings in the resource overheads, in particular, so-called quantum low-density parity-check (qLDPC) codes [6].

One recently discovered and promising class of qLDPC codes is *tile codes* [30, 16]. Tile codes were found by generalizing the surface code in the following way: Physical qubits are arranged on a square grid as for the surface code, but unlike for the surface code, stabilizer checks are allowed to have support inside a box of some fixed side length rather than being nearest-neighbor only. Hence, stabilizer checks can be non-planar, but they are local in the sense that they are supported within a constant-sized region. Such mild forms of non-locality would be accessible to hardware platforms with mobility, such as

*shinho.choe@meetiqm.com

†vincent.steffan@meetiqm.com

neutral-atom systems [15, 26, 1]. Recent developments in superconducting hardware also demonstrate that strict connectivity constraints can be relaxed [32, 25, 33, 2, 28, 27]. By construction, all stabilizer checks of tile codes are translationally invariant, so that the code is completely specified by the local set of checks and the boundaries. These restrictions allow for finding concrete examples by a brute-force computer search. In follow-up work it has been demonstrated that tile codes admit efficient protocols to implement logical gates [34] without any additional connectivity requirements and with moderate physical qubit overhead. In another follow-up work [22], concrete ways of implementing tile codes and other qLDPC code proposals like bivariate bicycle (BB) codes [19, 4, 9, 10, 7, 17, 18] on superconducting platforms have been investigated: According to [22], tile codes outperform all other investigated proposals for qLDPC codes significantly with respect to average coupler length and number of hardware components such as through-silicon vias, bump bonds and routing tiers.

While [30, 16] found several examples of codes with good parameters, there was little control over the structure of the codes. Their brute-force search is unsatisfactory from a purely theoretical viewpoint alone, but it is also problematic for the development of fault-tolerant logic, as this typically requires control over the logical operators. In the present work, we remedy this shortcoming twofold: First, we show that there exists a canonical choice of logical operators in tile codes. They are sets of pairs of associated X- and Z-logicals that only anti-commute with their partner. They can be localized along the boundary of the tile code, which makes them amenable to lattice surgery techniques. Interestingly, they arise naturally from the boundary conditions and are constructed via a cellular automaton rule, see Figure 1(a–c).

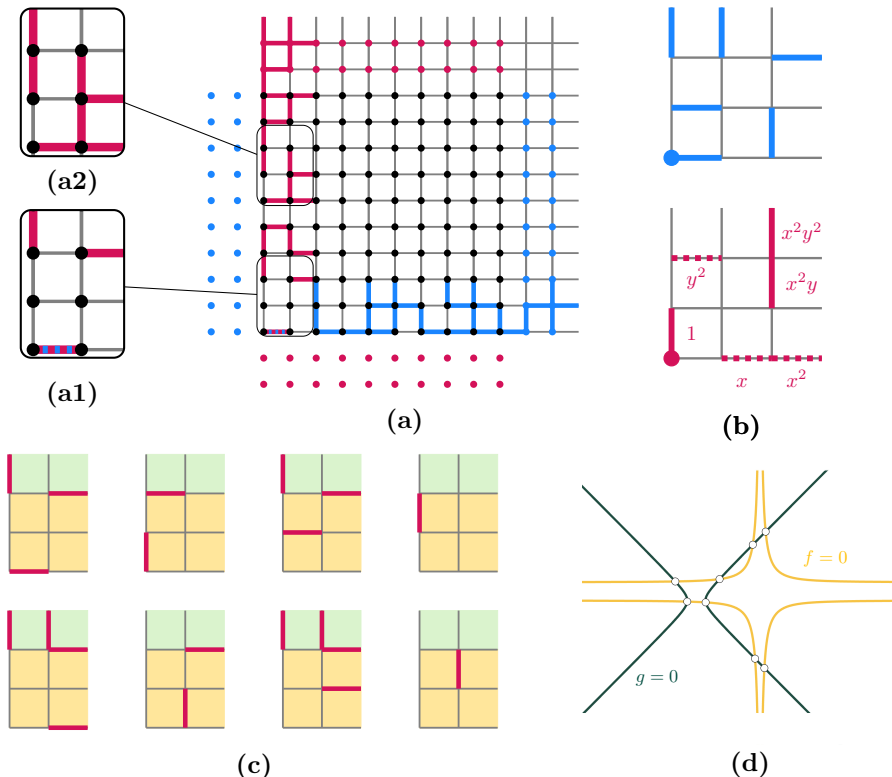


Figure 1: In (a), we show a tile code with a pair of logical operators \bar{X} and \bar{Z} . The stabilizer tiles for this code are shown in (b). The logical \bar{X} operators can be constructed using the cellular automaton depicted in (c). In (a1) and (a2), we highlight how the logical operator can be extended using linear combinations of the rules in (c). From an algebraic perspective, the logical dimension of a tile code corresponds to the number of intersection points of the zero sets of the polynomials defining the stabilizer tiles; for an illustration, see (e).

In the second part of the paper we introduce a framework that explains tile codes in the language of algebraic geometry: As it turns out, tile codes arise as higher global sections of a shifted Koszul complex

$$\mathcal{K}^\bullet(\mathbb{P}^1 \times \mathbb{P}^1, f, g) \otimes \mathcal{S} : \mathcal{O}(-2D, -2D) \otimes \mathcal{S} \xrightarrow{(-g, f)^t} \mathcal{O}(-D, -D)^2 \otimes \mathcal{S} \xrightarrow{(f, g)} \mathcal{O} \otimes \mathcal{S}$$

of vector bundles on $\mathbb{P}^1 \times \mathbb{P}^1$. Here, $f, g \in R = \mathbb{F}_2[x^\pm, y^\pm]$ is a pair of Laurent polynomials corresponding to the stabilizer tiles of the code, see Figure 1(b), while \mathcal{S} is a line bundle specifying the size of the bulk and the position of the X- and Z-boundary of the tile code. Using this algebro-geometric framework, we can show that the space of logicals of a tile code is isomorphic to $R/(f, g)$. In this way, the logical dimension of a tile code can be understood as the number of intersection points of the zero sets of f and g over \mathbb{F}_2 , see Figure 1 (d). This not only provides a different perspective on the structure of logical operators of tile codes, but also gives rise to an understanding of, e.g., tile codes in higher dimensions. For example, in Section 4 we explain how this lets one understand the structure of 4D versions of tile codes.

We then go on and introduce *derived automorphisms* for CSS codes inspired by derived categories. The notion of derived automorphisms for quantum codes is a relaxation of the usual automorphisms, which are permutations of qubits and stabilizer checks preserving the code space [13, 5, 10, 35]. Many codes do not allow for any automorphisms. For example, most tile codes have no automorphisms. We find that for tile codes, there are always derived automorphisms that can be implemented in a fault-tolerant manner with low qubit overhead. The action on the physical qubits consists of extending the tile code to one side and measuring out qubits on the opposite side. We show in Section 3.4 that this introduces a non-trivial circuit of CNOTs on the logical qubits whose action can be understood in terms of the cellular automaton mentioned before. Moreover, the action on logical operators can also be understood in terms of multiplication by x and y on $R/(f, g)$. We mention that this operation has been studied for the surface code in [11]: Here, since surface codes only have a single logical qubit, this action merely introduces a change in sign.

We believe that this work, which uses for the first time methods from homological algebra and algebraic geometry to study boundaries of qLDPC codes, opens the door for new research directions:

1. How can we optimally combine our low-overhead method of implementing CNOT circuits via derived automorphisms with other proposals for logical operations for tile codes, such as [34].
2. All results follow under some mild technical assumptions that we explain in Section 3. These assumptions are justified since all of the most efficient tile codes fulfill these assumptions [30]. Moreover, these assumptions turn out to hold in the ‘generic’ case, see Section 4. From a theoretical perspective, it might be interesting to also investigate the remaining corner-cases.
3. While first steps to study boundaries in qLDPC codes have been done in [18], our techniques make up the first systematic, formal exploration of boundaries in qLDPC codes using methods from homological algebra and algebraic geometry. We wonder how our techniques help understand boundary condensation phenomena and similar in the context of condensed matter physics.

The document is structured as follows: In Section 2, we recap the basics on stabilizer CSS codes from the perspective of homological algebra. In Section 3, we introduce stabilizer tiles on the 2D plane \mathbb{Z}^2 , recap the construction of tile codes as presented in [30], and present our main findings on the structure of logical operators of tile codes. There, we also present and introduce derived automorphisms for tile codes as an application. In Section 4, we explain how tile codes can alternatively be understood as resolutions of Koszul complexes. In Section 5 we give yet another way of explaining the structure of tile codes as Koszul complexes over $\mathbb{P}^1 \times \mathbb{P}^1$. We then discuss the concept of derived automorphisms for general CSS codes in Section 6.

2 Stabilizer CSS codes

A quantum CSS code $\mathcal{Q} \subset (\mathbb{C}^2)^{\otimes n}$ is the joint $+1$ eigenspace of a collection of commuting Pauli operators S_1, \dots, S_r where the operators S_i are elements of $\{\text{id}, X\}^{\otimes n} \cup \{\text{id}, Z\}^{\otimes n}$. Equivalently, we can specify the code by matrices $H_X \in \mathbb{F}_2^{r_X \times n}$ and $H_Z \in \mathbb{F}_2^{r_Z \times n}$ such that $H_X H_Z^{\text{tr}} = 0$. Here, the rows of H_X and H_Z correspond to the stabilizer generators S_i that are products of X and id and Z and id , respectively.

The matrices H_X and H_Z with $H_X H_Z^{\text{tr}} = 0$ can be viewed from a homological perspective. Namely, a chain complex C^\bullet of \mathbb{F}_2 -vector spaces equipped with bases

$$\dots \longrightarrow C^{i-1} \xrightarrow{d^{i-1}} C^i \xrightarrow{d^i} C^{i+1} \longrightarrow \dots$$

gives for each choice of index i a CSS code by taking H_X and H_Z^{tr} as the matrices associated to d^{i-1} and d^i .

This way, logical X-operators of the code \mathcal{Q} correspond to the first cohomology group $H^i(C^\bullet) = \ker(d^i) / \text{im}(d^{i-1})$ of the complex. The logical Z-operators can be identified with the dual space $H^i(C^\bullet)^*$.

Treating CSS codes as chain complexes allows us to import the language of homological algebra. For example, we will compare the spaces of logicals of various CSS codes via chain maps of the associated chain complexes. See for example [8], where several concepts from homological algebra are being used to study CSS codes.

3 Logical operators and derived automorphisms of tile codes

In this section, we will study tile codes and, in particular, the structure of logical operators of tile codes.

3.1 Stabilizer tiles on the 2D plane

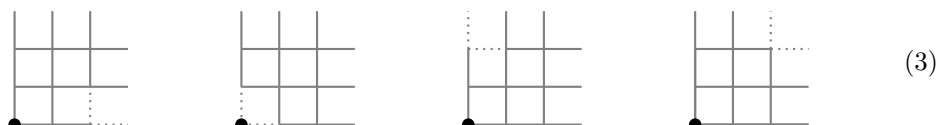
Consider the infinite 2D plane \mathbb{Z}^2 :



On each edge of the lattice sits a qubit. Each vertex of the lattice hosts one X-type and one Z-type *stabilizer tile* each in a translationally invariant fashion. Here, a X-type (resp. Z-type) stabilizer tile is a X-type (resp. Z-type) Pauli operator whose support is contained in a box of size $(D+1) \times (D+1)$ of which the south-west corner is the vertex at which the stabilizer tile is placed. We require that all X-type tiles and all Z-type tiles commute. An example of a valid pair of tiles with $D=2$ is the following:



We will always assume that $(D+1)$ is the minimal possible box size in which the stabilizer tile fits. More precisely, we will assume that the stabilizer tile always has support on at least one of the dotted edges in each of the following:



It will be handy to label nodes, horizontal edges, and vertical edges of the lattice \mathbb{Z}^2 by monomials in the Laurent polynomial ring $R_{\pm, \pm} = \mathbb{F}_2[x^\pm, y^\pm]$. In particular, we label

the node (a, b) , the horizontal edge connecting (a, b) with $(a + 1, b)$ and the vertical edge connecting (a, b) with $(a, b + 1)$ by $x^a y^b$ for any $a, b \in \mathbb{Z}$. In that way, any collection of X-tiles (resp. Z-tiles) can be specified by an element in $R_{\pm, \pm}$. Any finitely supported X-type (resp. Z-type) Pauli operator can be specified by a tuple $P = (P_h, P_v) \in R_{\pm, \pm}^2$.

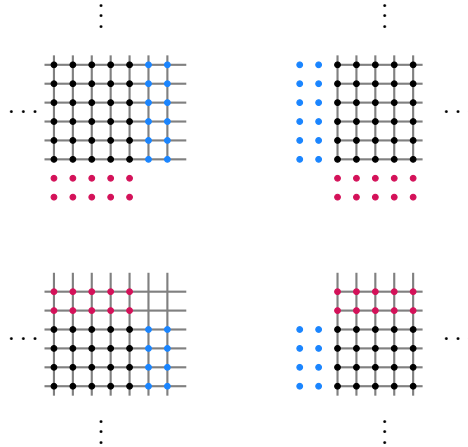
So, any choice of X-stabilizer tile as in Equation (2) corresponds to a pair of Laurent polynomials f, g . In this context, Equation (3) means that at least one of the polynomials has x -degree D and at least one of the two polynomials has y -degree D .

We will say that a Pauli Z-operator $P = (P_h, P_v)$ is *supported on a strip of length l* (resp. *on a strip of height m*) if there are no $(a, b), (\tilde{a}, \tilde{b}) \in P_h \cup P_v$ such that $|\tilde{a} - a| > l$ (resp. $|\tilde{b} - b| > m$). For example, the condition in Equation (3) ensures that the stabilizer tiles are not contained in strips of length or height D . More generally, the following simple observation will be helpful:

Lemma 1. *A non-empty product of stabilizers satisfying Equation (3) is never supported within a strip of height or width at most D .*

We say that the choice of stabilizer tiles gives rise to *topological order* (TO) if any finitely supported Pauli operator that commutes with all stabilizer tiles must itself be a product of stabilizer tiles¹. From now on, we will always assume TO.

Later, it will be helpful to define a stronger version of topological order, which we call *total topological order*. Assuming that a pair of stabilizer tiles is confined in boxes of size $(D + 1) \times (D + 1)$, the stabilizer tiles in the four quadrants all commute:



Here, we draw an edge for each qubit we include in the quadrant. A black dot indicates that the quadrant contains both an X- and a Z-type stabilizer tile at this position. Red dots (resp. blue dots) indicate that we only include an X-type (resp. Z-type) stabilizer at this position. Note that the supports of the red and blue stabilizer tiles are not entirely contained in the sublattice of qubits. In these cases, we will restrict the support of the tiles accordingly.

We say that the stabilizer tiles give rise to *total topological order* if, for each of the four quadrants depicted above, whenever a finitely supported Pauli operator commutes with all included stabilizers, then it must itself be a product of included stabilizers.

It will be useful to study excitations of the stabilizer tiles. We will only focus on excitations of Z-type stabilizer tiles; treating excitations of X-type stabilizer tiles works analogously. For a finitely supported X-type Pauli operator P , we call the element specifying the Z-type stabilizer tiles anticommuting with it the *syndrome* associated with P . We will write

$$\partial : R_{\pm, \pm} \oplus R_{\pm, \pm} \rightarrow R_{\pm, \pm} \tag{5}$$

¹The choice of tiles gives rise to a translationally invariant Pauli Hamiltonian with commuting terms on the 2D plane

$$H = - \sum_{x \in \mathbb{Z}^2} S_{X,x} - \sum_{z \in \mathbb{Z}^2} S_{Z,z}. \tag{4}$$

Here, $S_{X,x}$ and $S_{Z,z}$ are the X-type and Z-type stabilizer tiles at the vertex x and z respectively. Our notion of TO means that the ground space of this Hamiltonian exhibits TO.

for the map associating a syndrome $\partial(P)$ to a Pauli operator P . This map is often referred to as the *excitation map*. Then, TO means that if $\partial(P) = 0$, then P is a product of finitely many X-type stabilizer tiles.

3.2 Tile codes

Tile codes [9, 30, 16] are a systematic way of turning stabilizer tiles on the 2D plane \mathbb{Z}^2 into finite-size CSS codes. A tile code consists of a finite-size subset $\mathcal{T} \subset \mathbb{Z}^2$ of qubits and finite subsets of X-type and Z-type tiles such that all the stabilizer tiles we include, restricted to \mathcal{T} , commute. In this way, a tile code is a well-defined CSS code.

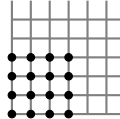
If the support of a tile is entirely contained in \mathcal{T} , we call it a *bulk stabilizer tile*. Else, we refer to it as a *boundary stabilizer tile*. We will refer to the stabilizer tiles whose support overlaps with \mathcal{T} but which are not included in the stabilizer set as *omitted boundary stabilizer tiles*.

We will now recap the construction consisting of four steps from [30]. For that, choose a valid pair of stabilizer tiles confined in boxes of size $(D+1) \times (D+1)$.

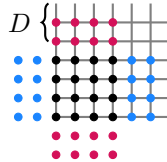
In **Step 1**, we choose a grid of bulk stabilizers of size $(L-D) \times (M-D)$, for example:



In **Step 2**, we draw the layout of qubits, which we choose to be the union of all $(D+1) \times (D+1)$ boxes that are centered at the vertices chosen in Step 1. This will result in a grid of $2LM$ many physical qubits.



In **Step 3**, we add boundary stabilizers. On the north and south side of the grid, we draw D layers of X-type gauge stabilizer tiles. On the east and west side of the grid, we draw D layers of Z-type gauge stabilizer tiles. Note that by the choice of qubit lattice, all included stabilizer tiles commute.



In **Step 4**, we delete qubits that are not supported by any X-type stabilizer (resp. Z-type stabilizer). If the support of a stabilizer is empty, we also delete that one. Finally, we add *corner stabilizers* if they commute with all so-far chosen stabilizers.

The best tile codes found so far in [30] were all constructed from tiles that satisfy Equation (3) and give rise to total topological order. They also came from constructions that terminated after the third step which turns out not to be a coincidence:

Lemma 2. *Say our stabilizer tiles satisfy condition Equation (3) and give rise to total topological order. Then, the construction terminates after Step 3.*

Proof. One easily checks that there are no qubits that are not supported by any X-type stabilizer (resp. Z-type stabilizer) by condition Equation (3). It is also clear that Equation (3) implies that all stabilizers have support on the lattice chosen in Step 2. Finally, total topological order implies that no corner term is commuting with all stabilizers. Hence, the tile code stays unchanged in Step 4. \square

Note that by Equation (3), the stabilizer generators of a tile code are independent. Since there are $2D^2$ more physical qubits than stabilizer generators, the logical dimension is $2D^2$. One can also say something about the logical dimension in the case where Equation (3) is not satisfied. This, however, is more involved, we touch upon this topic in Section 4.

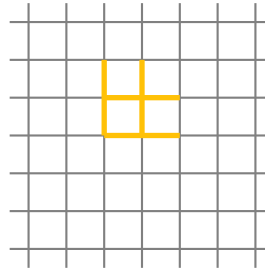
3.3 Logical operators of tile codes

In this section we will show that the tile codes admit a choice of basis of logical operators with many beneficial properties. We will first present our main findings and then give intuitive and visual, yet rigorous, proofs. For a visualization of Theorem 1 we refer to Figure 1.

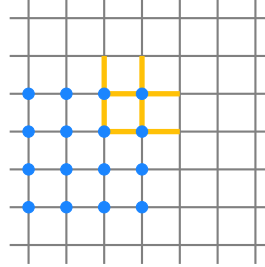
Theorem 1. *Consider a tile code constructed from stabilizer tiles confined in $(D+1) \times (D+1)$ boxes that satisfy Equation (3) and give rise to total topological order. Then, the following statements hold:*

1. *The tile code has a symplectic basis of logical operators labelled by the physical qubits in a $D \times D$ box in the bottom left corner. For each physical qubit in this box, exactly one pair of logical \bar{X} - and \bar{Z} -operators is supported there.*
2. *The logical operators of this symplectic basis can be chosen to live in strips of width (resp. height) D on the left (resp. bottom) of the tile code.*
3. *Within these strips, the representation of the logical operators is unique and can be constructed by a cellular automaton with a set of $2D^2$ rules.*
4. *All of these logical operators are products of omitted boundary stabilizers.*

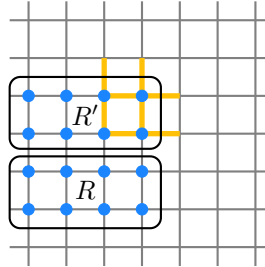
We will now, without loss of generality, study X-type operators. For Z-type operators, everything works analogously. Draw a box of size $D \times D$ on the lattice \mathbb{Z}^2 .



Any X-type Pauli operator whose support is contained in this box of size $D \times D$ can only anticommute with the Z-stabilizer tiles within the following region of width and height $2D$.



We split this set of Z-stabilizers into two regions R and R' , where R is the union of the D rows on the bottom and R' is the union of the D rows on the top.



Lemma 3. *Assuming total topological order, any X-type operator in the yellow box anticommutes with at least one stabilizer in R and at least one stabilizer in R' .*

Proof. Place the yellow box on the bottom left corner of the north-east quadrant. By condition Equation (3) and Lemma 1, no product of stabilizers of this quadrant is supported in this box. Hence, by total topological order, any X-type Pauli operator supported in the box must anticommute with some Z-type stabilizers of the quadrant. Since the stabilizers in R are discarded in this quadrant, there must be at least one stabilizer in R' anticommuting with the operator. Doing the same argument, putting the yellow box on the top right corner of the south-west quadrant, shows that there must be at least one Z-type stabilizer in R with which it anticommutes. \square

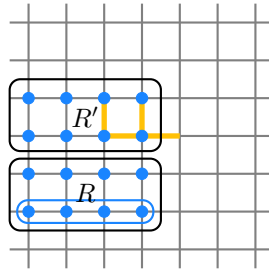
Corollary 1. *The $2D^2$ single qubit Pauli X-operators in the box give rise to linearly independent syndromes in both R and R' .*

Proof. If there would be a linear dependency then some non-trivial Pauli X-operator in the box does not trigger a syndrome. \square

Corollary 2. *Any syndrome in R (and any syndrome in R') can be triggered by a Pauli X-operator in the $D \times D$ -sized box.*

Proof. The space of syndromes in R (resp. in R') is $2D^2$ dimensional. Since the $2D^2$ different single qubit Pauli-X in the box trigger linearly independent syndromes they must span the whole space. \square

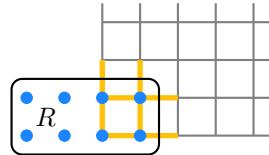
In fact, we know a little bit more than that. Consider only the bottom row of horizontal and vertical qubits of the yellow box:



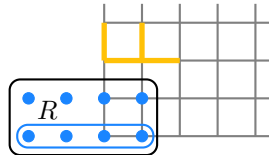
Then, the Pauli X-type operators on these $2D$ qubits yield linearly independent syndromes on the lowest row of Z-type stabilizers in R .

Corollary 3. *For all Pauli X-operators in the $D \times D$ box on the bottom left of a tile code there is a unique extension to a logical operator in a strip of width D .*

Proof. Pick any Pauli-X in the box on the bottom left.



We have seen that this Pauli X-operator may anticommute with some Z-type tile code stabilizers in the region R . But, we have also seen that there is a unique Z-operator in the following region highlighted in yellow triggering the same syndrome in the bottom row of R .



Extending the X-operator in the corner with this there is no syndrome in the bottom row of R left. Recursively, we find that there is a unique logical operator extending the Pauli X-operator on a strip such that there are no Z-checks violated. \square

We emphasize that this extension is unique not only up to stabilizers - there is only one logical operator representative in the strip continuing the pattern in the bottom left box. The proof of Corollary 3 in particular shows the following.

Corollary 4. *A tile code admits a symplectic basis of logical operators $\bar{X}_1, \bar{Z}_1, \dots, \bar{X}_D, \bar{Z}_D$ with the following properties:*

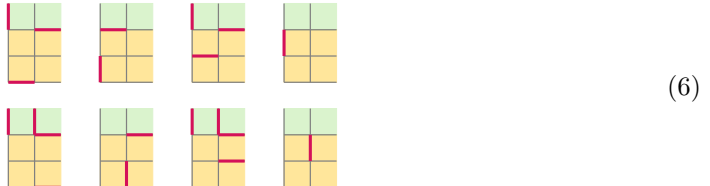
- *The pairs \bar{X}_i, \bar{Z}_i can be labelled by the physical qubits in the $D \times D$ box on the bottom left of the tile code in the sense that they are supported on this qubit and all other logicals in the symplectic basis are not.*
- *All \bar{X}_i are supported in a strip of width D along the left boundary of the tile code. All \bar{Z}_i are supported on a strip of height D on the bottom of the tile code.*

We depict an example of such a pair of logical operators in Figure 1 (a).

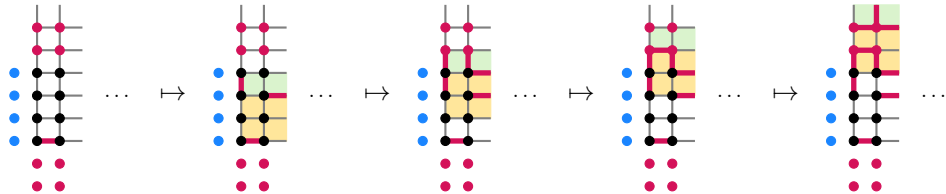
The proof of Corollary 3 shows that the elements of this symplectic basis arises from a cellular automaton. For more details on cellular automata we refer to [21]. We will now describe how to get the $2D^2$ rules that let one construct logical operators. Recall that any single qubit Pauli X_i in the green box gives rise to excited Z-type stabilizer tiles in R' . Let $a(X_i) = \prod_j X_j$ be the unique Pauli operator that excites the same syndrome in R' , in formulas, $\partial(X_i)|_{R'} = \partial(a(X_i))|_{R'}$.

Proposition 1. *The logical X- and Z-operators of the canonical symplectic basis in Corollary 4 can be constructed using a cellular automaton consisting of $2D^2$ rules each. The rules can be inferred from the paragraph above.*

For the stabilizer tiles in Equation (2), the 8 rules are as follows:



Let us illustrate in an example how to construct a logical operator step-by-step using this cellular automaton:



Here, in all steps except the first one, one has to apply linear combinations of the rules in Equation (6). For example, in the second step, one has to apply rules four and five. We also visualize the growing of logical operators via cellular automata in Figure 1.

The fact that logical operators can be easily understood in terms of cellular automata will be a crucial component for understanding so-called *derived automorphisms* in the next section.

We finish this section with some remarks regarding connections to other works.

Remark 1. *An alternative way of constructing a finite-size CSS code from translationally invariant Pauli stabilizer-tiles on the 2D plane is by introducing periodicity to construct so-called bivariate bicycle (BB) codes [4, 19]. The logical dimension of a BB code of a certain size turns out to be determined by the period of this cellular automaton.*

Remark 2. *For hypergraph product codes [31] a construction for a canonical basis of logical operators has been found in the past in [24]. In fact, it has been shown that hypergraph-product La-Cross codes [23, 9] are instances of tile codes where the stabilizers are induced by univariate polynomials. It turns out that for this special case these bases are the same when choosing the right pivot qubits in the method of [24].*

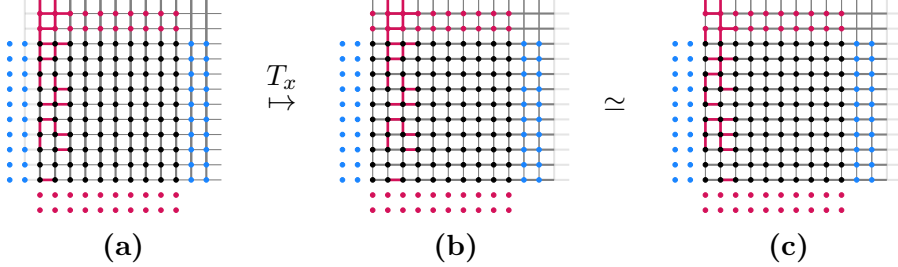


Figure 2: An example of a derived automorphism for a tile code: We track the logical operator \bar{X}_1 visualized in (a) where we stick to the labeling convention also used in Figure 1. By extending the lattice to the left and measuring out qubits on the right as described in Theorem 2, the logical operator \bar{X}_1 gets mapped to the logical operator in (b). Multiplying by stabilizers to bring this operator in canonical form, we easily see that this logical operator is equivalent to \bar{X}_5 .

Remark 3. *The concept of constructing logical operators via cellular automata is related to logical operators seen as fractal operators, see [14] for more details on fractal operators.*

The logical operators admit one more feature. We mention that this statement holds even when only assuming topological order and *total* topological order is not necessary. A statement similar to this was used in [34] to construct fault-tolerant logical operations on tile codes. For convenience of the reader, we state it here again.

Proposition 2. *Consider a Z-type logical operator \bar{Z} of a tile code. Then, \bar{Z} is the product of omitted boundary Z-stabilizers restricted to the tile code lattice.*

3.4 Derived automorphisms of tile codes

In this section, we define the *derived x- and y-automorphisms* T_x and T_y , which are logical Clifford operations on the tile codes that map X-operators to X-operators and Z-operators to Z-operators. Then, we explain how these operations can be implemented and how the basis constructed in Section 3.3 lets us understand the action on the encoded information. Derived automorphisms are a broader, new concept that we will discuss in more generality in Section 6. There, the choice of name will also become clear. We mention that the notion of derived automorphisms for quantum codes is a relaxation to the usual automorphisms, which are permutations of qubits and stabilizer checks preserving the code space [13, 5, 10, 35]. In this section, we will only discuss how derived automorphisms can be understood for tile codes; for a more general discussion, we refer to Section 6.

We define the derived *x-automorphism* T_x by the action on the logical operators. First, we define its action on the logical X-operator. By Corollary 4, without loss of generality, we may assume that any logical X-operator is fully supported in the strip of width D along the left boundary. We define the action of T_x on the logical X-operators by shifting its support by +1 in the *x*-direction, see Figure 2.

Next, we define the action of T_x on the logical Z-operators. By Corollary 4, we may assume without loss of generality that a non-trivial logical Z-operator \bar{Z} is supported in the strip of width D along the bottom boundary. As an intermediate step, we obtain \bar{Z}_{shifted} by first shifting \bar{Z} by +1 in the *x* direction and then restricting to the tile code lattice.



By construction, the Pauli \bar{Z}_{shifted} supports none of the D qubits (yellow in Equation (7)) at the bottom left vertical strip of the lattice. We construct the desired logical operator $T_x(\bar{Z})$ by extending \bar{Z}_{shifted} to include some Pauli Z on the vertical strip. The product becomes a logical operator if and only if the D syndromes (red in Equation (7)) are trivial. By

Corollary 1, one can always find a unique extension of \bar{Z}_{shifted} such that the extended Pauli is a logical operator.

The derived y automorphism T_y is defined analogously to T_x where we swap the roles of X and Z as well as the x - and y -direction. It turns out that the derived automorphism preserves symplecticity of the logical basis.

Proposition 3. *For our symplectic basis $\bar{X}_1, \bar{Z}_1, \dots$ constructed in Theorem 1, the set $T_x(\bar{X}_1), T_x(\bar{Z}_1), \dots$ is again a symplectic basis of the space of logical operators.*

Proof. It is clear by construction that since $\langle \bar{X}_i, \bar{Z}_j \rangle = \delta_{ij}$ also $\langle T_x(\bar{X}_i), T_x(\bar{Z}_j) \rangle = \delta_{ij}$ holds. Moreover, by construction, it is clear that all $T_x(\bar{X}_i)$ and $T_x(\bar{Z}_j)$ commute with all stabilizers of the tile code. This finishes the proof. \square

One can implement T_x^ϵ for $\epsilon = \pm 1$ on a tile code state by “sliding” a tile code in the x direction. The procedure is precisely described in the following theorem. For a visualization, see Figure 2.

Theorem 2. *Suppose we apply the following operations to a tile code state $|\psi\rangle$ on the lattice \mathcal{L} .*

(P1) *Extend the lattice by adding one column on the left-hand side (resp. right-hand side) if $\epsilon = 1$ or $\epsilon = -1$, respectively, and prepare ancilla qubits on the edges in the new column as $|0\rangle$. Denote \mathcal{L}^+ the extended lattice.*

(P2) *Measure all X -stabilizer generators of the new tile code defined on the extended lattice.*

(P3) *Measure the qubits at the right (resp. left) columns if $\epsilon = 1$ (resp. $\epsilon = -1$) in Z -basis. Denote the subset of the measured qubits whose measurement outcome is -1 by M . Denote \mathcal{L}' the shifted lattice obtained by removing edges of the measured qubits from the extended lattice \mathcal{L}^+ .*

(P4) *Denote $(\bar{X}'_i, \bar{Z}'_i)_{i=1}^k$ the logical operators on the shifted lattice \mathcal{L}' obtained by translating the logical operators (\bar{X}_i, \bar{Z}_i) of the original lattice \mathcal{L} . Apply the logical operators $\prod_{i=1}^k \bar{X}'_i^{j_i}$ of the tile code on the shifted lattice where $j_i = 0$ if the overlap $|M \cap \text{supp}(\bar{Z}_i)|$ of M and the support of \bar{Z}_i is even, and $j_i = 1$ otherwise.*

Then, the output state is a logical state $T_x^\epsilon |\psi\rangle$ of the tile code defined on the shifted lattice \mathcal{L}' up to a Pauli frame update which is determined by the measurement outcomes of (P2) and (P3).

Proof. We only give a proof for the case with $\epsilon = 1$. The case with $\epsilon = -1$ works analogously.

For the proof, we track the stabilizer group of the logical state $|\psi\rangle$. We first consider the case where $|\psi\rangle$ is a ± 1 eigenstate of the logical \bar{Z} -operators. Denote \mathcal{S}_X and \mathcal{S}_Z the sets of X - and Z -type tile code stabilizer generators on the original lattice. The stabilizer group of $|\psi\rangle$ is generated by

$$\mathcal{S}_X \cup \mathcal{S}_Z \cup \{\sigma_1 \bar{Z}_1, \dots, \sigma_k \bar{Z}_k\} \quad \text{with} \quad \sigma_1, \dots, \sigma_k \in \{-1, 1\}. \quad (8)$$

Denote \mathcal{A} the set of ancilla qubits and Z_a for $a \in \mathcal{A}$ the Pauli Z -operator at the qubit a in (P1). The stabilizer group of the entire state after (P1) is generated by

$$\mathcal{S}_X \cup \mathcal{S}_Z \cup \{\sigma_1 \bar{Z}_1, \dots, \sigma_k \bar{Z}_k\} \cup \{Z_a\}_{a \in \mathcal{A}}. \quad (9)$$

Denote \mathcal{S}_X^+ and \mathcal{S}_Z^+ the X -and Z -type tile code stabilizer generators on the extended lattice \mathcal{L}^+ . It is clear by construction that $\mathcal{S}_Z \cup \{Z_a\}_{a \in \mathcal{A}}$ and $\tilde{\mathcal{S}}_Z \cup \{Z_a\}_{a \in \mathcal{A}}$ generate the same Pauli subgroup. We also replace the logical operators \bar{Z}_i with the unique extension $\bar{Z}_i^+ := P_i \bar{Z}_i$ where Z -type Pauli P_i is the multi-qubit Z -Pauli supported on the ancilla qubits \mathcal{A} such that \bar{Z}_i^+ is a logical Z -operator on the extended lattice \mathcal{L}^+ . Therefore, we can write the generating set in Equation (9) as

$$\mathcal{S}_X \cup \mathcal{S}_Z^+ \cup \{\sigma_1 \bar{Z}_1^+, \dots, \sigma_k \bar{Z}_k^+\} \cup \{Z_a\}_{a \in \mathcal{A}}. \quad (10)$$

In (P2), we measure all stabilizers in the set $\mathcal{S}_X^+ \setminus \mathcal{S}_X$, which is the set of X-stabilizers at the left boundary of the extended lattice, as well as the tile code stabilizers \mathcal{S}_X of the original lattice \mathcal{L} . We observe how the generating subset $\{Z_a\}_{\mathcal{A}}$ evolves during the measurement procedure. Indeed, the generating subset $\{Z_a\}_{\mathcal{A}}$ is transformed into a set of multi-qubit Pauli Z-operators which are supported on the left boundary and commute with all X-stabilizers of the extended lattice \mathcal{L}^+ . By the total topological order condition, those Pauli Z-operators must be Z-stabilizers of the extended lattice. Therefore, the stabilizer group of the state on the entire system after (P2), ignoring the sign in front of the stabilizers in $\mathcal{S}^+ \setminus \mathcal{S}$ caused by the measurement result, is generated by

$$\mathcal{S}_X^+ \cup \mathcal{S}_Z^+ \cup \{\sigma_1 \bar{Z}_1^+, \dots, \sigma_k \bar{Z}_k^+\}. \quad (11)$$

Now, we observe how the stabilizer group in Equation (11) evolves in (P3). Using the argument analogous to that showing how the generating subset $\{Z_a\}$ evolves to a subset of \mathcal{S}_Z^+ , one can show that the generating subset \mathcal{S}_X^+ evolves to \mathcal{S}'_X , the set of X-stabilizers on the shifted lattice \mathcal{L}' . Note also that \mathcal{S}_Z^+ evolves into \mathcal{S}'_Z when we ignore the sign of the stabilizers caused by the single-qubit measurement result. One can also see from the definition of the derived automorphism T_x that the logical operator \bar{Z}_i^+ and the single-qubit Paulis on the measured qubits generate $(-1)^{|M \cap \text{supp}(\bar{Z}_i)|} T_x(\bar{Z}_i)$. Therefore, the stabilizer group of the state on the remaining qubit after (P3) is generated by

$$\mathcal{S}'_X \cup \mathcal{S}'_Z \cup \{(-1)^{|M \cap \text{supp}(\bar{Z}_i)|} \sigma_i T_x(\bar{Z}_i)\}_{i=1}^k. \quad (12)$$

After applying the logical operator $\prod_{i=1}^k \bar{X}_i^{j_i}$ in (P4), the stabilizer group has the generating set

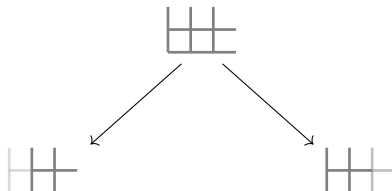
$$\mathcal{S}'_X \cup \mathcal{S}'_Z \cup \{\sigma_1 T_x(\bar{Z}_1), \dots, \sigma_k T_x(\bar{Z}_k)\}. \quad (13)$$

In an analogous way, one can track stabilizers assuming that the initial tile code state is an eigenstate of logical X operators. This finishes the proof. \square

This protocol is exactly the tile code version of moving a patch of surface code used in lattice surgery protocols [11, 20]. We note that another method of deforming a tile code, involving both extending and shrinking, also appears in the logical Pauli measurement protocol of Ref. [34]. Unlike Theorem 2, they include only a selection of X-stabilizer tiles (resp. Z-stabilizer tiles): In this way, they gauge products of logical operators of the code and are able to measure these products in that way.

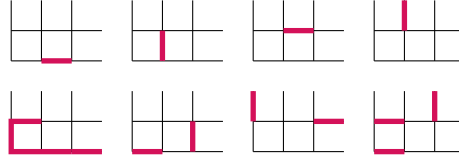
Similarly as for the surface code, the sliding protocol can also be implemented in a fault-tolerant way with the following modification. In (P2), we measure Z stabilizers of the extended lattice as well, and we repeat the measurement d times, where d is the minimal distance of the tile code. After (P3), we measure X and Z stabilizers of the shifted code d times again. Since stabilizers of the original code are products of Pauli Z-operators in M and boundary stabilizers in the slid version, the parity of $|M \cap \text{supp}(\bar{Z})|$ can be reliably inferred even in the presence of measurement errors.

Remark 4. *The action of the protocol described in Theorem 2 on the logical operators can also be understood as a cellular automaton: Using topological order, one can see that for any X-type operator supported on a $D \times D$ box, there is a unique way of extending the support to the left to make it commute with one additional row of stabilizers.*



With that, for the two tiles in Equation (2), the following eight patterns completely

describe the action of T_x . This can again be interpreted as a cellular automaton.



An example of a whole logical operator being moved one step to the left can be seen in Figure 2. There, the first rule of this cellular automaton is being applied. This idea will be made more formal in Section 4.

Example 1. We can track the action of T_x on all logical X- and Z-operators of the tile code whose stabilizer tiles are those in Equation (2). The action on logical operators can be described by two matrices

$$T_x = \begin{pmatrix} A & 0 \\ 0 & B \end{pmatrix} \in \mathbb{F}_2^{16 \times 16}, A = \begin{pmatrix} 0 & 0 & 0 & 0 & 1 & 1 & 0 & 1 \\ 0 & 0 & 0 & 0 & 1 & 0 & 0 & 0 \\ 0 & 0 & 0 & 0 & 1 & 0 & 0 & 1 \\ 0 & 0 & 0 & 0 & 0 & 0 & 1 & 0 \\ 1 & 0 & 0 & 0 & 1 & 0 & 0 & 0 \\ 0 & 1 & 0 & 0 & 0 & 0 & 0 & 0 \\ 0 & 0 & 1 & 0 & 0 & 0 & 1 & 0 \\ 0 & 0 & 0 & 1 & 0 & 0 & 0 & 0 \end{pmatrix}, B = \begin{pmatrix} 0 & 0 & 0 & 0 & 0 & 0 & 1 & 0 & 0 \\ 1 & 0 & 0 & 0 & 0 & 1 & 0 & 0 & 1 \\ 0 & 0 & 0 & 0 & 0 & 0 & 1 & 0 & 1 \\ 0 & 0 & 1 & 0 & 0 & 0 & 0 & 1 & 0 \\ 1 & 0 & 0 & 0 & 0 & 0 & 0 & 0 & 0 \\ 0 & 1 & 0 & 0 & 0 & 0 & 0 & 0 & 0 \\ 0 & 0 & 1 & 0 & 0 & 0 & 0 & 0 & 0 \\ 0 & 0 & 0 & 1 & 0 & 0 & 0 & 0 & 0 \end{pmatrix},$$

where the columns of A and B represent $T_x(\bar{X}_i)$ and $T_x(\bar{Z}_i)$.

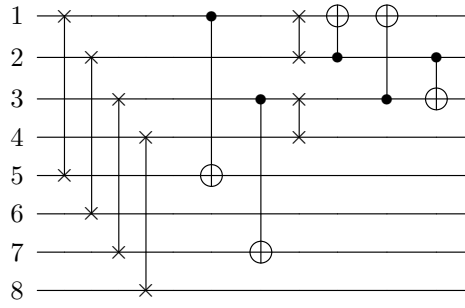
Analogously, one can calculate the action of T_y on the logical operators. The matrix form of the automorphism T_y is

$$T_y = \begin{pmatrix} C & 0 \\ 0 & D \end{pmatrix} \in \mathbb{F}_2^{16 \times 16}, C = \begin{pmatrix} 1 & 0 & 0 & 1 & 0 & 0 & 0 & 1 \\ 0 & 0 & 1 & 0 & 0 & 0 & 0 & 0 \\ 1 & 0 & 0 & 0 & 0 & 0 & 0 & 0 \\ 0 & 1 & 0 & 0 & 0 & 0 & 0 & 0 \\ 0 & 0 & 0 & 0 & 1 & 0 & 0 & 1 \\ 0 & 0 & 0 & 1 & 0 & 0 & 1 & 0 \\ 0 & 0 & 0 & 0 & 1 & 0 & 0 & 0 \\ 0 & 0 & 0 & 0 & 0 & 1 & 0 & 0 \end{pmatrix}, D = \begin{pmatrix} 0 & 0 & 0 & 1 & 0 & 0 & 0 & 1 & 0 \\ 0 & 0 & 1 & 0 & 0 & 0 & 0 & 0 & 0 \\ 1 & 0 & 0 & 1 & 0 & 0 & 0 & 1 & 0 \\ 0 & 1 & 0 & 0 & 0 & 0 & 0 & 0 & 0 \\ 0 & 0 & 0 & 1 & 0 & 0 & 0 & 1 & 1 \\ 0 & 0 & 0 & 0 & 0 & 0 & 1 & 0 & 0 \\ 0 & 0 & 0 & 1 & 1 & 0 & 0 & 1 & 1 \\ 0 & 0 & 0 & 0 & 0 & 0 & 0 & 0 & 0 \end{pmatrix},$$

where the columns of C and D represent $T_y(\bar{X}_i)$ and $T_y(\bar{Z}_i)$.

One can see that $T_y = T_x^{150}$ and they generate the same cyclic subgroup of $\mathrm{Sp}(16, \mathbb{F}_2)$ of order 217. This can be understood more rigorously from an algebraic perspective, see Example 2.

From the matrices A and B , one can easily construct a circuit composed of logical CNOT and SWAP gates that is actually implemented by T_x :



4 Homological algebra of tile codes

In this section, we describe how tile codes can be ‘resolved’ by infinite dimensional codes, that arise as Koszul complexes in (Laurent)-polynomial rings.

4.1 Background on Koszul complexes

For a commutative ring R and elements $f, g \in R$, the *Koszul complex* is defined as

$$K(R, f, g)^\bullet : R \xrightarrow{(-g, f)^t} R^2 \xrightarrow{(f, g)} R \quad (14)$$

By convention, the terms in the complex are in cohomological degrees $-2, -1$ and 0 . One can show that the cohomology groups of the Koszul have the following form [10]

$$H^i(K(R, f, g)^\bullet) \cong \begin{cases} R/(f, g) & \text{if } i = 0, \\ \frac{(f) \cap (g)}{(fg)} & \text{if } i = -1, \\ \text{ann}_R(f) \cap \text{ann}_R(g) & \text{if } i = -2 \text{ and} \\ 0 & \text{otherwise.} \end{cases}$$

Here, we denote by $(r_1, \dots, r_n) \subset R$ the ideal generated by n elements $r_1, \dots, r_n \in R$. Moreover, we denote by $\text{ann}_R(r) = \{s \in R \mid rs = 0\}$ the annihilator of $r \in R$.

Recall that elements $f, g \in R$ form a *Koszul-regular sequence*, if

$$H^i(K(R, f, g)^\bullet) = 0 \text{ for } i = -2, -1.$$

So $f, g \in R$ are a Koszul-regular sequence if and only if the Koszul complex $K(R, f, g)^\bullet$ is a resolution of $R/(f, g)$.

We are particularly interested in the case that $f, g \neq 0$ and R is a unique factorization domain, so for example a (Laurent)-polynomial ring over a field. In this case, we always have that $H^{-2}(K(R, f, g)^\bullet) = 0$. Hence, $f, g \in R$ form a Koszul-regular sequence if and only if $(f) \cap (g) = (fg)$ which is equivalent to the statement that f and g have no (non-unit) common divisors in R .

We will also need Koszul complexes in the following slightly more general form. Assume that $f : R_1 \rightarrow R$ and $g : R_2 \rightarrow R$ are maps of a free rank one R -modules to R , then we obtain the Koszul complex

$$K(R, f, g)^\bullet : R_1 \otimes_R R_2 \xrightarrow{(-1 \otimes g, f \otimes 1)^t} R_1 \oplus R_2 \xrightarrow{(f, g)} R \quad (15)$$

By choosing identifications of R_1, R_2 with R , this is isomorphic to the above definition. However, it will be useful for us in order to take care of certain shifts.

4.2 Codes on infinite lattices as Koszul complexes

We will now explain in detail how Koszul complexes are related to the CSS codes on a $2D$ -plane, as introduced in Section 3. For this, we consider the (Laurent)-polynomial rings

$$R_{\epsilon_1 \epsilon_2} = \mathbb{F}_2[x^{\epsilon_1}, y^{\epsilon_2}] \text{ for } \epsilon_1, \epsilon_2 \in \{+, -, \pm\}. \quad (16)$$

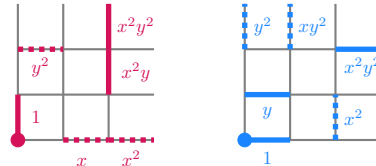
For example, $R_{\pm -} = \mathbb{F}_2[x^{\pm 1}, y^{-1}]$. These rings naturally have a basis by monomials $x^a y^b$ which we can identify with coordinates $(a, b) \in \mathbb{Z}^2$. Moreover, we abbreviate $R = R_{\pm \pm}$.

To obtain the CSS code on the unbounded infinite $2D$ -plane, Equation (1), we consider the Koszul complex

$$K^\bullet = K^\bullet(R, f, g) : R \xrightarrow{(g, f)^t} R^2 \xrightarrow{(f, g)} R.$$

The basis vectors of the terms $K^i(R, f, g)$ in the correspond to the coordinates of X-checks, vertical/horizontal qubits and Z-checks, for $i = -2, -1$ and 0 , respectively.

The polynomials f, g specify the stabilizer tiles in the following way. The vertical and horizontal qubits in the X-tile correspond to f and g , respectively, while the vertical and horizontal qubits in the Z-tile correspond to $(xy)^D g(x^{-1}, y^{-1})$ and $(xy)^D f(x^{-1}, y^{-1})$, respectively. The fact that the stabilizer tiles are confined within a box of size B is equivalent to the assumption that $f, g \in \mathbb{F}_2[x, y]$ are polynomials of maximal degree $D = B - 1$ in both x and y . For example, the polynomials $f = 1 + x^2 y + x^2 y^2$ and $g = x + x^2 + y^2$, correspond to the stabilizer tiles



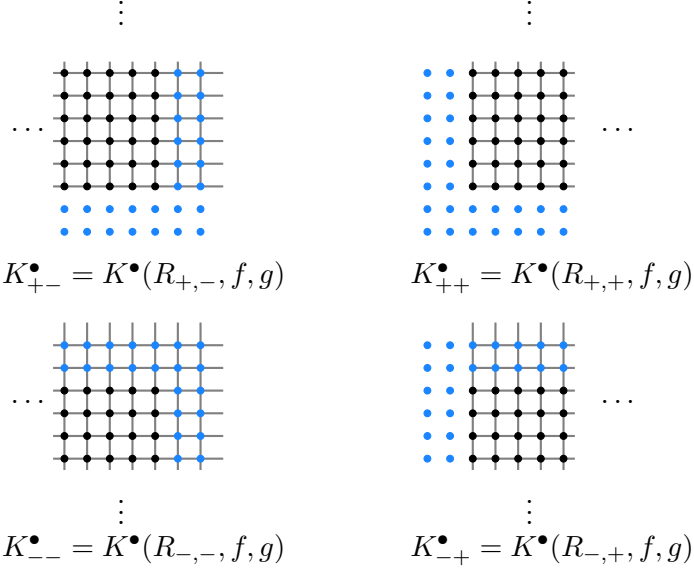


Figure 3: Koszul complexes and associated CSS codes supported on the four different quadrants.

Moreover, we mention that the excitation map ∂ defined in Equation (5) can be identified with the differential (f, g) in the Koszul complex.

Similarly to the Koszul complex corresponding to the the unbounded infinite plane discussed above, we also consider Koszul complexes $K_{\epsilon_1 \epsilon_2}^\bullet$ associated to coordinate quadrants and half planes by using the rings $R_{\epsilon_1 \epsilon_2}$ for $\epsilon_i \in \{\pm, +, -\}$.

For example, the Koszul complex

$$K_{++}^\bullet = K^\bullet(R, f, g) : R_{++} \xrightarrow{(g, f)^t} R_{++}^2 \xrightarrow{(f, g)} R_{++}$$

corresponds to a CSS code supported on the right-upper quadrant, see Figure 3.

Whenever $\epsilon_1 = -$ and or $\epsilon_2 = -$, the polynomials f, g are no longer elements in $R_{\epsilon_1 \epsilon_2}$ and we need to incorporate a shift. For this, define

$$s_{\epsilon_1 \epsilon_2} = x^{-D(\epsilon_1)} y^{-D(\epsilon_2)}$$

where $D(\epsilon) = D$ if $\epsilon = -$ and $D(\epsilon) = 0$, else. Then, multiplication with f, g yields a map $s_{\epsilon_1 \epsilon_2} R_{\epsilon_1 \epsilon_2} \rightarrow R_{\epsilon_1 \epsilon_2}$. We then obtain the Koszul complex, see Equation (15),

$$K_{\epsilon_1 \epsilon_2}^\bullet = K(R, f, g) : s_{\epsilon_1 \epsilon_2}^2 R_{\epsilon_1 \epsilon_2} \xrightarrow{(g, f)^t} s_{\epsilon_1 \epsilon_2} R_{\epsilon_1 \epsilon_2}^2 \xrightarrow{(f, g)} R_{\epsilon_1 \epsilon_2}. \quad (17)$$

See Figure 3 for the corresponding CSS codes on the four quadrants.

With this definition, we will now define an algebraic analog of the topological order conditions considered in Section 3. Namely, we say that the polynomials f, g satisfy *algebraic topological order* if for all $\epsilon_1, \epsilon_2 \in \{+, -, \pm\}$ we have

1. $H^i(K_{\epsilon_1 \epsilon_2}) = 0$ for all $i \neq 0$ and
2. the map $R_{\epsilon_1 \epsilon_2}/(s_{\epsilon_1 \epsilon_2} f, s_{\epsilon_1 \epsilon_2} g) \rightarrow R/(f, g)$ is an isomorphism.

Remark 5. 1. The first condition holds if and only if $s_{\epsilon_1 \epsilon_2} f, s_{\epsilon_1 \epsilon_2} g$ form a Koszul-regular sequence in $R_{\epsilon_1 \epsilon_2}$ or, equivalently, if $s_{\epsilon_1 \epsilon_2} f, s_{\epsilon_1 \epsilon_2} g$ have no common non-unit factors in $R_{\epsilon_1 \epsilon_2}$.

2. The second condition is equivalent to $x^{-\epsilon_1}, y^{-\epsilon_2} \in \mathbb{F}_2[x^{\epsilon_1}, y^{\epsilon_2}]/(s_{\epsilon_1 \epsilon_2} f, s_{\epsilon_1 \epsilon_2} g)$.

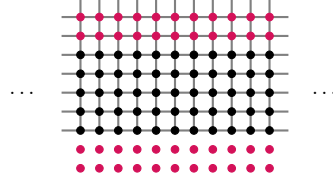
We will assume this algebraic topological order from now. In fact, one may show that this implies total topological order defined in Section 3.1. One can verify that all tile codes found in [30] obey algebraic topological order.

4.3 Resolving tile codes by Koszul complexes

We now explain how the tile codes introduced in Section 3.2 can be constructed via an ‘inclusion-exclusion principle’ using the Koszul complexes on the unbounded infinite plane, half planes and quadrants, as well as shifts thereof.

For this, we will use the various natural inclusions of the different Koszul complexes. For example, there is a natural map $y^k K_{++} \rightarrow K_{\pm, \pm}$ which maps the upper-right quadrant, shifted up by k steps, into the right half plane.

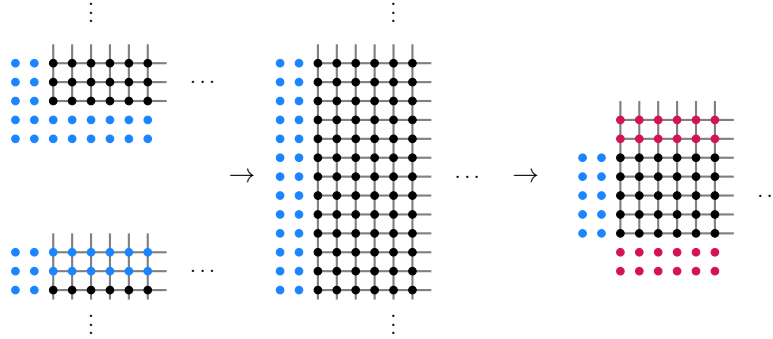
In a first approximation, we consider codes supported on a horizontal strips, which are either bounded to the left, bounded to the right or unbounded in the horizontal direction. For example, the unbounded strip has the following form.



Strip codes of height M arise from the following short exact sequence of chain complexes

$$0 \longrightarrow y^{M+D} K_{\epsilon,+}^\bullet \oplus y^{D-1} K_{\epsilon,-}^\bullet \longrightarrow K_{\epsilon,\pm}^\bullet \longrightarrow K_{\epsilon,\text{strip}}^\bullet \longrightarrow 0. \quad (18)$$

For example, the strip code bounded to the left, arises by removing two quadrants from a half-plane, as the following picture shows.



We will now show how this resolution on strip codes allows to compute their logical operators.

Lemma 4. *Let $\epsilon \in \{+, -, \pm\}$. Then $H^i(K_{\epsilon,\text{strip}}^\bullet) = 0$ for all $i \neq -1$ and there is an isomorphism*

$$\partial_{\text{bottom}} : H^{-1}(K_{\epsilon,\text{strip}}^\bullet) \rightarrow R/(f, g)$$

defined by

$$\partial_{\text{bottom}}([a, b]) = \text{tr}_{y < 0}(af + bg) \in R/(f, g)$$

for a representative (a, b) of a cohomology class. Here, for a polynomial h , we denote by $\text{tr}_{y < 0}(h)$ the polynomial that arises by setting all non-negative powers of y in h to zero.

Proof. For ease of notation, assume that $\epsilon = \pm$. The other cases follow by the same argument. The algebraic total order condition implies that $H^i(K_{\pm\epsilon}^\bullet) = 0$ for $i \neq 0$ and that the maps $H^0(K_{\pm\epsilon}^\bullet) \rightarrow H^0(K_{\pm\pm}^\bullet) = R/(f, g)$ are isomorphism for all $\epsilon' \in \{+, -\}$. This implies that the long exact sequence of cohomology groups associated to the short exact sequence in Equation (18) has the following form

$$0 \longrightarrow H^{-1}(K_{\pm,\text{strip}}^\bullet) \xrightarrow{\delta} H^0(K_{\pm,-}^\bullet) \oplus H^0(K_{\pm,+}^\bullet) \xrightarrow{\pi} H^0(K_{\pm\pm}^\bullet) \longrightarrow 0$$

and all other terms vanish. In particular, $H^i(K_{\epsilon,\text{strip}}^\bullet) = 0$ for all $i \neq -1$.

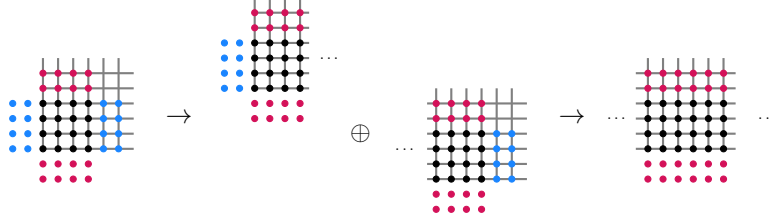
Since both components of the map π , namely $H^0(K_{\pm-}^\bullet) \rightarrow H^0(K_{\pm\pm}^\bullet)$ and $H^0(K_{\pm+}^\bullet) \rightarrow H^0(K_{\pm\pm}^\bullet)$, are isomorphism by algebraic topological order, it follows that both components of the boundary map δ are isomorphism as well. In particular, the boundary map δ composed with the projection to $H^0(K_{\pm-})$ yields the desired isomorphism

$$\partial_{\text{bottom}} : H^{-1}(K_{\text{tile}}^\bullet) \rightarrow H^0(K_{\pm-}) \cong R/(f, g). \quad \square$$

Finally, the tile code arises from the following short exact sequence

$$0 \longrightarrow K_{\text{tile}}^\bullet \longrightarrow K_{+ \text{strip}}^\bullet \oplus x^{L+D} K_{- \text{strip}}^\bullet \longrightarrow K_{\pm \text{strip}}^\bullet \longrightarrow 0. \quad (19)$$

Visually, this means that the tile code is the intersection of the two (shifted) strip codes bounded to the left and right, respectively, inside the unbounded strip code.



This resolutions of tile codes via strip codes allows to identify the space of logicals of tile codes and strip codes.

Lemma 5. *The inclusion $K_{\text{tile}}^\bullet \rightarrow K_{\pm \text{strip}}^\bullet$ is a quasi-isomorphism, that is, it induces an isomorphism $H^i(K_{\text{tile}}^\bullet) \rightarrow K_{\pm \text{strip}}^\bullet$ for all $i \in \mathbb{Z}$.*

Proof. Using Lemma 4, the inclusion $K_{+ \text{strip}}^\bullet \rightarrow K_{\pm \text{strip}}^\bullet$ and $x^{L+D} K_{+ \text{strip}}^\bullet \rightarrow K_{\pm \text{strip}}^\bullet$ are quasi-isomorphisms and the long exact sequence associated to the short exact sequence of chain complexes in Equation (19) is given by

$$\begin{array}{ccccccc} 0 & \longrightarrow & H^{-1}(K_{\text{tile}}^\bullet) & \longrightarrow & H^{-1}(K_{+ \text{strip}}^\bullet) \oplus H^{-1}(x^{L+D} K_{- \text{strip}}^\bullet) & \longrightarrow & H^{-1}(K_{\pm \text{strip}}^\bullet) \longrightarrow 0 \\ & & \downarrow \wr & & \downarrow \wr & & \downarrow \wr \\ 0 & \longrightarrow & R/(f, g) & \xrightarrow{(\text{id}, \text{id})^t} & R/(f, g) \oplus R/(f, g) & \xrightarrow{(\text{id}, \text{id})} & R/(f, g) \longrightarrow 0 \end{array}$$

where the right vertical maps are given by the map ∂_{bottom} as defined in Lemma 4. \square

Putting together Lemma 4 and Lemma 5, we obtain the following explicit description of the space of logicals of the tile code.

Theorem 3. *We have $H^i(K_{\text{tile}}^\bullet) = 0$ for all $i \neq -1$ and the map $\partial_{\text{bottom}} : H^{-1}(K_{\text{tile}}^\bullet) \rightarrow R/(f, g)$ defined as in Lemma 4 is an isomorphism.*

With this result, we can immediately compute the logical dimension.

Theorem 4. *The logical dimension of a tile code is given by*

$$\dim_{\mathbb{F}_2} H^{-1}(K_{\text{tile}}^\bullet) = \dim_{\mathbb{F}_2} R/(f, g) = 2D^2.$$

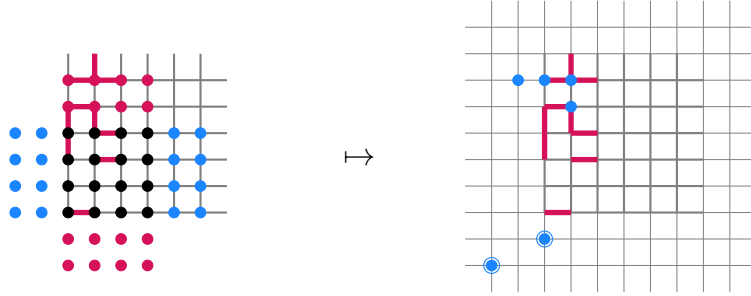
Proof. Since $H^{-2}(K_{\text{tile}}^\bullet) = H^0(K_{\text{tile}}^\bullet) = 0$, the logical dimension is given by

$$\begin{aligned} \dim_{\mathbb{F}_2} H^{-1}(K_{\text{tile}}^\bullet) &= \dim_{\mathbb{F}_2} K_{\text{tile}}^{-1} - \dim_{\mathbb{F}_2} K_{\text{tile}}^0 - \dim_{\mathbb{F}_2} K_{\text{tile}}^{-2} \\ &= 2LM - (L+D)(M-D) - (L-D)(M+D) = 2D^2 \end{aligned}$$

as claimed. \square

The effect of the map ∂_{bottom} on an X-logical P in a tile code can be visualised as follows. First, one embeds the logical operator into a the infinite grid. Second, one computes the boundary exitation $\partial(P)$, that is, the set of coordinates of Z-stabilizers in the infinite grid

that anti-commute with P . These excitations are localized along the top and bottom boundary of the tile code, as the following picture visualizes.



Third, we disregard the top boundary excitations. The remaining bottom boundary excitations can then be interpreted as a Laurent polynomial $\partial_{\text{bottom}}(P) \in R$. To make this construction invariant under adding X-stabilizers to P we mod out the ideal generated by f, g and obtain $\partial_{\text{bottom}}(P) \in R/(f, g)$.

Analogously to the relations between strip codes extending in the horizontal direction, one may also consider vertical strip codes, say $K_{\pm \text{strip}}^{\bullet}$. Then the projection map $K_{\pm \text{strip}}^{\bullet} \rightarrow K_{\text{tile}}^{\bullet}$ which sends all qubits and checks to zero that are not in the tile code is a quasi-isomorphism as well. This can be shown by a similar argument.

Remark 6. *Combining the two short exact sequences in Equation (18) and in Equation (19) yields the following double complex*

$$C^{\bullet, \bullet} : C^{0, \bullet} \longrightarrow C^{1, \bullet} \longrightarrow C^{2, \bullet}$$

built from the Koszul complexes on the quadrants, half planes and the unbounded infinite plane

$$\begin{aligned} C^{0, \bullet} &= y^{M+D} K_{++}^{\bullet} \oplus x^{L+D} y^{M+D} K_{-+}^{\bullet} \oplus y^{D-1} K_{+-}^{\bullet} \oplus x^{L+D} y^{D-1} K_{--}^{\bullet}, \\ C^{1, \bullet} &= y^{M+D} K_{\pm+}^{\bullet} \oplus y^{D-1} K_{\pm-}^{\bullet} \oplus K_{+\pm}^{\bullet} \oplus x^{L+D} K_{-\pm}^{\bullet} \text{ and} \\ C^{2, \bullet} &= K_{\pm, \pm}^{\bullet}. \end{aligned}$$

where the differentials in the vertical direction increasing the first index in $C^{\bullet, \bullet}$ are given by the natural inclusion maps and the horizontal differentials are given by the differentials in the Koszul complexes. The tile code complex $K_{\text{tile}}^{\bullet}$ arises as the vertical cohomology of the double complex $C^{\bullet, \bullet}$, namely,

$$H_{\rightarrow}^i(C^{\bullet, \bullet}) = \begin{cases} K_{\text{tile}}^{\bullet} & \text{if } i = 1 \text{ and} \\ 0 & \text{otherwise.} \end{cases}$$

Here, by $H_{\rightarrow}^i(C^{\bullet, \bullet})$ we denote the complex that arises by taking the i -th cohomology along the vertical differential in the double complex $C^{\bullet, \bullet}$.

In this way, the double complex $C^{\bullet, \bullet}$ can be seen as a ‘resolution’ of the tile code complex. In fact, the double complex $C^{\bullet, \bullet}$ naturally arises as the Čech complex computing the higher global section of a Koszul complex on $\mathbb{P}^1 \times \mathbb{P}^1$ that we will discuss in the next section.

5 Geometry of tile codes

We will now explain how tile codes arise naturally when considering Koszul complex on the variety $\mathbb{P}^1 \times \mathbb{P}^1$. We assume some familiarity with algebraic geometry.

5.1 Line bundles and Koszul complexes on $\mathbb{P}^1 \times \mathbb{P}^1$

We first introduce some basic facts and notations for line bundles on \mathbb{P}^1 . Since we are interested in CSS codes, so chain complexes over \mathbb{F}_2 , we always denote by $\mathbb{P}^1 = \mathbb{P}_{\mathbb{F}_2}^1$ the projective line over \mathbb{F}_2 .

Recall that (up to isomorphism) all line bundles on \mathbb{P}^1 are of the form $\mathcal{O}(n)$ for $n \in \mathbb{Z}$ where $\mathcal{O}(0) = \mathcal{O}$ is the trivial line bundle. The global sections on the line bundle $\mathcal{O}(n)$ arise as rational functions on \mathbb{P}^1 that are defined everywhere but at ∞ and are allowed to have a pole of order of up to n at ∞ , or in other words, polynomials of degree bounded by n ,

$$\Gamma(\mathbb{P}^1, \mathcal{O}(n)) = \begin{cases} \mathbb{F}_2[x]_{\leq n} & \text{for } n \geq 0 \text{ and} \\ 0 & \text{otherwise.} \end{cases} \quad (20)$$

While the line bundles $\mathcal{O}(n)$ for $n < 0$ have no non-trivial global sections, they have (except for $n = -1$) higher global sections given by

$$R^1\Gamma(\mathbb{P}^1, \mathcal{O}(n)) = \begin{cases} (\mathbb{F}_2[x]_{\leq -n-2})^* & \text{for } n < -1 \text{ and} \\ 0 & \text{otherwise.} \end{cases} \quad (21)$$

Moreover, all other higher global sections vanish

$$R^i\Gamma(\mathbb{P}^1, \mathcal{O}(n)) = 0 \text{ for all } i > 1.$$

We will now explain how this generalizes to $\mathbb{P}^1 \times \mathbb{P}^1$. Here, we will use the variables x and y for the first and second copy of \mathbb{P}^1 , respectively.

Line bundles on $\mathbb{P}^1 \times \mathbb{P}^1$ arise from line bundles on each copy of \mathbb{P}^1 and are given by $\mathcal{O}(n_1, n_2) = \mathcal{O}(n_1) \boxtimes \mathcal{O}(n_2)$ for two integers n_1, n_2 . The (higher) sections of these line bundles can be computed via the Künneth formula

$$R^i\Gamma(\mathbb{P}^1 \times \mathbb{P}^1, \mathcal{O}(n_1, n_2)) = \bigoplus_{\substack{0 \leq p, q \leq 1 \\ p+q=i}} R^p\Gamma(\mathbb{P}^1, \mathcal{O}(n_1)) \otimes_{\mathbb{F}_2} R^q\Gamma(\mathbb{P}^1, \mathcal{O}(n_2)), \quad (22)$$

where $R^0\Gamma = \Gamma$. For example, if $D \geq 0$, then we obtain polynomials in x, y of maximal degree D in both x and y as global sections

$$\Gamma(\mathbb{P}^1 \times \mathbb{P}^1, \mathcal{O}(D, D)) = \mathbb{F}_2[x]_{\leq D} \otimes_{\mathbb{F}_2} \mathbb{F}_2[y]_{\leq D} = \mathbb{F}_2[x, y]_{\leq D, \leq D}.$$

Morphisms between line bundles can be computed via

$$\begin{aligned} \text{Hom}(\mathcal{O}(n_1, n_2), \mathcal{O}(m_1, m_2)) &= \text{Hom}(\mathcal{O}, \mathcal{O}(m_1 - n_1, m_2 - n_2)) \\ &= \Gamma(\mathbb{P}^1 \times \mathbb{P}^1, \mathcal{O}(m_1 - n_1, m_2 - n_2)). \end{aligned}$$

In particular, if we choose $f, g \in \mathbb{F}_2[x, y]_{\leq D, \leq D}$, we obtain the Koszul complex

$$\mathcal{K}^\bullet(\mathbb{P}^1 \times \mathbb{P}^1, f, g) : \mathcal{O}(-2D, -2D) \xrightarrow{(g, f)^t} \mathcal{O}(-D, -D)^2 \xrightarrow{(f, g)} \mathcal{O}. \quad (23)$$

concentrated in degrees $-2, -1, 0$.

If we identify the vector bundles with their sheaves of sections, we can consider the cohomology sheaves of the Koszul complex. For example, the 0-th cohomology sheaf is

$$H^0(\mathcal{K}^\bullet(\mathbb{P}^1, f, g)) = \mathcal{O}/(f, g),$$

the sheaf of functions on the joint vanishing set of the polynomials f, g in $\mathbb{P}^1 \times \mathbb{P}^1$.

5.2 Local Sections and codes on infinite lattices

We now explain how the Koszul complexes in Equation (17) considered in Section 4.2 can be recovered from the Koszul complex of vector bundles on $\mathbb{P}^1 \times \mathbb{P}^1$ (Equation (23)). For this, we consider the following open affine subsets of the projective line

$$\mathbb{A}_+^1 = \mathbb{P}^1 - \{\infty\}, \mathbb{A}_-^1 = \mathbb{P}^1 - \{0\} \text{ and } \mathbb{A}_\pm^1 = \mathbb{G}_m = \mathbb{A}_+^1 \cap \mathbb{A}_-^1 = \mathbb{P}^1 - \{0, \infty\}.$$

Here \mathbb{A}_+^1 and \mathbb{A}_-^1 are copies of the affine line \mathbb{A}^1 .

The space of sections into the line bundles $\mathcal{O}(n)$ over these subsets is given by

$$\Gamma(\mathbb{A}_+^1, \mathcal{O}(n)) = \mathbb{F}_2[x], \Gamma(\mathbb{A}_-^1, \mathcal{O}(n)) = x^n \mathbb{F}_2[x^{-1}] \text{ and } \Gamma(\mathbb{A}_\pm^1, \mathcal{O}(n)) = \mathbb{F}_2[x^\pm] \quad (24)$$

so that the sections over \mathbb{P}^1 arise as intersection

$$\Gamma(\mathbb{P}^1, \mathcal{O}(n)) = \Gamma(\mathbb{A}_+^1, \mathcal{O}(n)) \cap \Gamma(\mathbb{A}_-^1, \mathcal{O}(n)) = \mathbb{F}_2[x] \cap x^n \mathbb{F}_2[x^{-1}].$$

By taking products, we obtain open affine subsets of $\mathbb{P}^1 \times \mathbb{P}^1$ of the form

$$\mathbb{A}_{\epsilon_1 \epsilon_2}^2 = \mathbb{A}_{\epsilon_1}^1 \times \mathbb{A}_{\epsilon_2}^1 \subset \mathbb{P}^1 \times \mathbb{P}^1$$

for $\epsilon_i \in \{+, -, \pm\}$. The spaces of sections into the line bundles $\mathcal{O}(n_1, n_2)$ can be computed via Equation (24) and

$$\Gamma(\mathbb{A}_{\epsilon_1 \epsilon_2}^2, \mathcal{O}(n_1, n_2)) = \Gamma(\mathbb{A}_{\epsilon_1}^1, \mathcal{O}(n_1)) \otimes_{\mathbb{F}_2} \Gamma(\mathbb{A}_{\epsilon_2}^1, \mathcal{O}(n_2))$$

In particular, we obtain the various (Laurent)-polynomial rings defined in Equation (16) as functions over these subspaces $R_{\epsilon_1 \epsilon_2} = \Gamma(\mathbb{A}_{\epsilon_1 \epsilon_2}^2, \mathcal{O})$ and the Koszul complexes in Equation (17) arise as sections of the Koszul complex in Equation (23),

$$K_{\epsilon_1 \epsilon_2}^\bullet = \Gamma(\mathbb{A}_{\epsilon_1 \epsilon_2}^2, \mathcal{K}^\bullet(\mathbb{P}^1 \times \mathbb{P}^1, f, g)). \quad (25)$$

Using these facts, one shows that the algebraic topological order condition is equivalent to the following *geometric total topological order* condition that

1. $H^i(\mathcal{K}^\bullet(\mathbb{P}^1, f, g)) = 0$ for $i \neq 0$ and
2. the restriction map $\Gamma(\mathbb{P}^1 \times \mathbb{P}^1, \mathcal{O}/(f, g)) \rightarrow \Gamma(\mathbb{A}_{\pm\pm}^2, \mathcal{O}/(f, g)) = R/(f, g)$ is an isomorphism.

The second condition is equivalent to the condition that the f and g do not vanish simultaneously at either $x = 0, \infty$ or $y = 0, \infty$, which is ensured by the condition in Equation (3).

5.3 Tile codes as higher sections

We now explain how tile codes arise naturally as higher sections of a shift of the Koszul complex $\mathcal{K}^\bullet(\mathbb{P}^1 \times \mathbb{P}^1, f, g)$, see Equation (23). For this, for integers L, M defining the size of the tile code, we consider the shifted Koszul complex

$$\mathcal{K}_{\text{tile}} := \mathcal{K}^\bullet(\mathbb{P}^1 \times \mathbb{P}^1, f, g) \otimes \mathcal{S}$$

where $\mathcal{S} = \mathcal{O}(L - 1 + D, -M - 1 + D)$. The resulting complex is explicitly given by

$$\mathcal{O}(L - 1 - D, -M - D) \xrightarrow{(g, f)^t} \mathcal{O}(L - 1, -M)^2 \xrightarrow{(f, g)} \mathcal{O}(L - 1 + D, -M + D)$$

where we apologize for the unwieldy numbers.

Using the Künneth formula, see Equation (22), and computation of higher sections of line bundles on \mathbb{P}^1 , see Equation (20) and Equation (21), one can check that the complex K_{tile}^\bullet arises as the higher global $R^1\Gamma(\mathbb{P}^1 \times \mathbb{P}^1, -)$ of the entries of the shifted Koszul complex $\mathcal{K}_{\text{tile}}$,

$$\begin{array}{ccccccc} R^1\Gamma(\mathbb{P}^1 \times \mathbb{P}^1, \mathcal{K}_{\text{tile}}^{-2}) & \longrightarrow & R^1\Gamma(\mathbb{P}^1 \times \mathbb{P}^1, \mathcal{K}_{\text{tile}}^{-1}) & \longrightarrow & R^1\Gamma(\mathbb{P}^1 \times \mathbb{P}^1, \mathcal{K}_{\text{tile}}^0) \\ \parallel & & \parallel & & \parallel \\ K_{\text{tile}}^{-2} & \longrightarrow & K_{\text{tile}}^{-1} & \longrightarrow & K_{\text{tile}}^0 \end{array}$$

We observe that the choice of the line bundle \mathcal{S} determines the $L \times M$ -shape of the tile code as well as the positioning of the ‘smooth’ and ‘rough’ boundaries according to the positive and negative sign in front of L and M .

With this geometric approach, one can easily recover the computations of logicals of tile codes from Theorem 3. The geometric total topological order condition implies that the complex $\mathcal{K}_{\text{tile}}$ is quasi-isomorphic to the complex $\mathcal{O}/(f, g) \otimes \mathcal{S}$ concentrated in degree 0.

By the geometric total topological order condition, we obtain that

$$\begin{aligned} R^n\Gamma(\mathbb{P}^1 \times \mathbb{P}^1, \mathcal{O}/(f, g) \otimes \mathcal{S}) &= R^n\Gamma(\mathbb{A}_{\pm\pm}^2, \mathcal{O}/(f, g) \otimes \mathcal{S}) \\ &= R^n\Gamma(\mathbb{A}_{\pm\pm}^2, \mathcal{O}/(f, g)) = \begin{cases} R/(f, g) & \text{for } n = 0 \text{ and} \\ 0 & \text{otherwise.} \end{cases} \end{aligned}$$

Here the second equality uses that all line bundles on $\mathbb{A}_{\pm\pm}^2$ are trivial and the higher sections vanish since $\mathbb{A}_{\pm\pm}^2$ is affine.

We can now consider the spectral sequence

$$E_1^{p,q} = R^q\Gamma(\mathbb{P}^1 \times \mathbb{P}^1, \mathcal{K}_{\text{tile}}^p) \Rightarrow R^{p+q}(\mathbb{P}^1 \times \mathbb{P}^1, \mathcal{O}/(f, g) \otimes \mathcal{S})$$

associated to the stupid filtration of the complex $\mathcal{K}_{\text{tile}}$ which compares the higher sections of the terms of the complex $\mathcal{K}_{\text{tile}}$ to the higher sections of the complex itself, see [29].

Now, using the computations of higher global sections in Equation (20), Equation (21) and Equation (22), one obtains that $E_1^{p,q} = 0$ for $p \neq 0$ and $q \neq -2, -1, 0$. In fact, the non-trivial terms on the first page E_1 together with the differential are exactly equal to the complex $\mathcal{K}_{\text{tile}}^\bullet$, see Section 5.3.

This shows that the spectral sequence degenerates at page 2, which contains the cohomology groups of the tile code complex. We hence obtain in total

$$H^q(\mathcal{K}_{\text{tile}}^\bullet) = E_2^{1,q} = R^{1+q}\Gamma(\mathbb{P}^1 \times \mathbb{P}^1, \mathcal{O}/(f, g) \otimes \mathcal{S}) = \begin{cases} R/(f, g) & \text{for } q = -1 \text{ and} \\ 0 & \text{otherwise.} \end{cases}$$

Remark 7. In Theorem 4, we show that the logical dimension of tile codes is $2D^2$. By this, we essentially reproved Bezout's theorem which states that the number of intersection points of curves described by equations $f = 0$ and $g = 0$ in $\mathbb{P}^1 \times \mathbb{P}^1$ can be computed as

$$\dim H^0(\mathbb{P}^1 \times \mathbb{P}^1, \mathcal{O}/(f, g)) = \deg_X f \deg_y g + \deg_y f \deg_X g.$$

Here, \deg_X and \deg_y denotes the degree of f and g in the variables x and y , respectively. By our assumption, all these degrees are equal to D and we obtain a logical dimension of $2D^2$.

5.4 Increasing the dimension

The geometric interpretation of tile codes as higher global section in a shifted Koszul complex on $\mathbb{P}^1 \times \mathbb{P}^1$ opens the way to a systematic construction of open boundary versions of translation invariant systems in any dimension, say $n \geq 0$.

For example, we can construct three-dimensional tile codes using $X = \mathbb{P}^1 \times \mathbb{P}^1 \times \mathbb{P}^1$. The shape of the stabilizers will be described by three polynomials

$$f, g, h \in \mathbb{F}_2[x, y, z]_{\leq D, \leq D, \leq D} = \Gamma(X, \mathcal{O}(D, D, D))$$

To this, we can associate a three-term Koszul complex in degrees $-3, \dots, 0$ given by

$$\mathcal{K}(X, f, g, h) : \mathcal{L}^{\otimes 3} \xrightarrow{\begin{pmatrix} g \\ f \\ h \end{pmatrix}} (\mathcal{L}^{\otimes 2})^3 \xrightarrow{\begin{pmatrix} h & 0 & g \\ 0 & h & f \\ f & g & 0 \end{pmatrix}} \mathcal{L}^3 \xrightarrow{(f \ g \ h)} \mathcal{O}$$

where we denote the line bundle $\mathcal{L} = \mathcal{O}(-D, -D, -D)$. We choose to put X-stabilizers, qubits and Z-stabilizers in degrees $-2, -1$ and 0 , respectively. The shape of the layout of the resulting code can be determined by the choice of an additional line bundle \mathcal{S} , so that we consider the complex of vector bundles

$$\mathcal{K}_{3D\text{-tile}} = \mathcal{K}(X, f, g, h) \otimes \mathcal{S}$$

and define the three dimensional tile code via the space of higher sections

$$K_{3D\text{-tile}}^\bullet : R^1\Gamma(X, \mathcal{K}_{3D\text{-tile}}^{-2}) \longrightarrow R^1\Gamma(X, \mathcal{K}_{3D\text{-tile}}^{-1}) \longrightarrow R^1\Gamma(X, \mathcal{K}_{3D\text{-tile}}^0).$$

We choose the line bundle \mathcal{S} such that $R^i\Gamma(X, \mathcal{S})$ is only non-zero for $i = 1$. For example, for

$$\mathcal{S} = \mathcal{O}(L - 1 + D, M - 1 + D, -N + D)$$

we will obtain a code with qubits supported on the $3LMN$ edges of a cube with Z-boundaries on the boundaries in the x, y -directions and X-boundaries in the z -direction, corresponding to the choice of signs. When we assume the appropriate generalization of geometric total topological order, the space of logicals of the code can be computed as

$$H^{-1}(K_{3D\text{-tile}}^\bullet) \cong \mathbb{F}_2[x^{\pm 1}, y^{\pm 1}, z^{\pm 1}]/(f, g, h)$$

and one may show that the dimension of the space of logicals is $6D^3$.

Similarly, we can construct four-dimensional tile codes using $X = \mathbb{P}^1 \times \mathbb{P}^1 \times \mathbb{P}^1 \times \mathbb{P}^1$. The shape of the stabilizers will be described by four polynomials

$$f, g, h, i \in \mathbb{F}_2[w, x, y, z]_{\leq D, \leq D, \leq D, \leq D} = \Gamma(X, \mathcal{O}(D, D, D, D)).$$

To this, we can associate a Koszul complex $\mathcal{K}(X, f, g, h, i)$. The most natural choice is to put X-stabilizers, qubits and Z-stabilizers in the middle degrees degrees $-3, -2$ and -1 , respectively, where the Koszul complex has the form

$$(\mathcal{L}^{\otimes 3})^4 \xrightarrow{\begin{pmatrix} h & g & 0 & f & 0 & 0 \\ i & 0 & g & 0 & f & 0 \\ 0 & i & h & 0 & 0 & f \\ 0 & 0 & 0 & i & h & g \end{pmatrix}^t} (\mathcal{L}^{\otimes 2})^6 \xrightarrow{\begin{pmatrix} g & h & i & 0 & 0 & 0 \\ f & 0 & 0 & h & i & 0 \\ 0 & f & 0 & g & 0 & i \\ 0 & 0 & f & 0 & g & h \end{pmatrix}} (\mathcal{L})^4$$

for $\mathcal{L} = \mathcal{O}(-D, -D, -D, -D)$. We choose the line bundle $\mathcal{S} = \mathcal{O}(L - 1 + D, M - 1 + D, -N + D, -P + D)$ and define shifted Koszul complex $\mathcal{K}_{4D\text{-tile}} = \mathcal{K}(X, f, g, h, i) \otimes \mathcal{S}$. Passing to the second derived higher sections, we obtain the complex

$$K_{4D\text{-tile}}^\bullet : R^2\Gamma(X, \mathcal{K}_{4D\text{-tile}}^{-3}) \longrightarrow R^2\Gamma(X, \mathcal{K}_{4D\text{-tile}}^{-2}) \longrightarrow R^2\Gamma(X, \mathcal{K}_{4D\text{-tile}}^{-1}).$$

The resulting code is supported on a hypercube with $6LMNP$ qubits supported on the faces. When we assume the appropriate generalization of geometric total topological order, the space of logicals of the code can be computed as

$$H^{-1}(K_{4D\text{-tile}}^\bullet) \cong \mathbb{F}_2[w^{\pm 1}, x^{\pm 1}, y^{\pm 1}, z^{\pm 1}]/(f, g, h, i)$$

and one may show that the dimension of the space of logicals is $24D^4$. For example, choosing $D = 1, L = M = N = P = 3$ as well as polynomials

$$\begin{aligned} f &= 1 + xy + wyz + wxz + x, & g &= xz + w + wxy + wxyz + z, \\ h &= yz + x + wz + wy + wxy, & i &= z + y + xyz + wx + wxz, \end{aligned}$$

we obtain a code with parameters $[[486, 24, 10 \leq d \leq 15]]$.

6 Derived Automorphisms

We introduce the notion of derived automorphisms of CSS codes and discuss it in the example of tile codes. This gives the theoretical backbone to the derived automorphisms construct ad-hoc in Section 3.4.

6.1 Definition

In this section, we introduce a generalized notion of isomorphism of CSS codes, that naturally encapsulates the derived automorphisms considered in Section 3.4, but might also be of independent interest.

For this, we first discuss a complication in the definition of a morphism of CSS codes. It might be tempting to define a morphism between two CSS codes as chain maps between the associated chain complexes, say C^\bullet and C'^\bullet . However, that this introduces a very unnatural asymmetry, since the X- and Z-parity checks of the CSS codes are treated in an asymmetric

way in the associated chain complexes. For this reason, it seems to be reasonable to rather consider certain *correspondences* between the chain complexes, that is, diagrams of the form

$$\begin{array}{ccc} & D^\bullet & \\ C^\bullet & \swarrow & \searrow \\ & C'^\bullet & \end{array}$$

where D^\bullet is a third chain complex and the two arrows are chain maps. In particular, correspondences can be transposed by simply switching the role of C^\bullet and C'^\bullet . This effectively removes the asymmetry. Now, based on the application, one can put various restriction on the chain maps in the correspondence, for example regarding the preservation of distance or bases.

Secondly, it can be very valuable to weaken the notion of isomorphism. Recall that a chain map $C^\bullet \rightarrow D^\bullet$ is called a *quasi-isomorphism* if it induces an isomorphism on all cohomology groups $H^i(C^\bullet) \xrightarrow{\sim} H^i(D^\bullet)$. For example, adding a single qubit and a check that is supported on this qubit yields a quasi-isomorphic code. Another example is the inclusion of the tile code in a code supported on a horizontal strip, see Lemma 5.

Combining these two ideas, we define a *derived isomorphism* between to CSS codes given by chain complexes C^\bullet and C'^\bullet as a diagram of the form

$$\begin{array}{ccccccc} & D_1^\bullet & & D_2^\bullet & & D_n^\bullet & \\ q.i. \swarrow & & q.i. \searrow & q.i. \swarrow & q.i. \searrow & q.i. \swarrow & \\ C^\bullet & & C_1^\bullet & & \dots & & C'^\bullet \end{array}$$

where all arrows are quasi-isomorphisms. Derived isomorphism can be composed by concatenation of their diagrams. While in the diagram defining a derived automorphism, the maps go out of the objects D_i^\bullet , one may turn this around by the following construction:

$$\begin{array}{ccccc} & C^\bullet & & C'^\bullet & \\ \equiv & \searrow & & \swarrow & \equiv \\ C^\bullet & & D^\bullet & & C'^\bullet \end{array}$$

A *derived automorphism* is a derived isomorphism between the same chain complex $C^\bullet = C'^\bullet$. We note that if C^\bullet is quasi-isomorphic to C'^\bullet , then each automorphism of C'^\bullet yields a derived automorphism of C^\bullet .

We will mostly be interested in derived isomorphisms that fulfill two additional conditions. First, we assume that all chain complexes in the diagram are equipped with bases and all chain maps send each basis vector either to a unique basis vector or to zero. Second, we assume that the distance of C_i^\bullet and $C_i'^\bullet$ is at least the distance of C^\bullet and C'^\bullet . With these assumptions, one may construct a fault-tolerant circuit that implements a derived isomorphism.

Remark 8. As suggested by the name, derived isomorphism are closely related to isomorphisms in the derived category of \mathbb{F}_2 -vector spaces. However, in this category each complex is isomorphic to a complex with trivial differential and hence a trivial code. So, it is important to impose restrictions on the allowed chain maps.

6.2 Derived automorphism of tile codes

As in Section 4.3 we denote by K_{tile}^\bullet denote the chain complex associated to a tile code defined by polynomials f, g . We assume that the polynomials fulfill algebraic topological order, see Section 4.2. In particular, this implies that the space of logical operators is given by

$$H^{-1}(K_{\text{tile}}^\bullet) = R/(f, g) = \mathbb{F}_2[x^\pm, y^\pm]/(f, g).$$

While, in general, a tile code has no automorphism that sends basis vectors to basis vectors due to the open boundary condition, we will now realize multiplication by x and y as derived automorphisms, say T_x and T_y . Moreover, we show that their action on the space of logicals is given by multiplication on $R/(f, g)$.

A quick way to see this that however involves infinite dimensional codes is the following. Multiplication by x yields an automorphism of $K_{\pm, \text{strip}}^\bullet$, say T_x , which acts by multiplication by x on $H^{-1}(K_{\pm, \text{strip}}^\bullet) = R/(f, g)$. The natural inclusion yields a quasi-isomorphism

$K_{\text{tile}}^\bullet \rightarrow K_{\pm, \text{strip}}^\bullet$, and we obtain the desired derived automorphism T_x of K_{tile}^\bullet . The derived automorphism T_y is obtained similarly by using the quasi-isomorphism $K_{\text{strip}, \pm}^\bullet \rightarrow K_{\text{tile}}^\bullet$ and the action of y on $K_{\text{strip}, \pm}^\bullet$.

These derived automorphism can also be realized using only finite dimensional codes. One can obtain the derived automorphism T_x using the diagram

$$\begin{array}{ccc} K_{\text{tile}}^\bullet & \searrow & K_{\text{tile}}^\bullet \\ & K'_{\text{tile}}^\bullet & \swarrow \end{array}$$

where K'_{tile}^\bullet is a tile code of size $(L + 1) \times M$. The first map embeds the copy of the tile code K_{tile}^\bullet of size $L \times M$ on the left side of K'_{tile}^\bullet . The second map embeds K_{tile}^\bullet on the right side of K'_{tile}^\bullet .

Similarly, the derived automorphism T_y also arises from the diagram

$$\begin{array}{ccc} & K''_{\text{tile}}^\bullet & \\ \swarrow & & \searrow \\ K_{\text{tile}}^\bullet & & K_{\text{tile}}^\bullet \end{array}$$

where $K''_{\text{tile}}^\bullet$ is a tile code of size $L \times (M + 1)$ and the two maps remove the top (respectively bottom) row of qubits and checks in $K''_{\text{tile}}^\bullet$.

This gives exactly the derived automorphisms that we constructed in Section 3.4 by extending the lattice and measuring out qubits.

The group generated by the derived automorphism T_x and T_y now depends on the polynomials f, g . We close the section with explaining the structure observed in Example 1 from an algebraic perspective.

Example 2. *We can now understand Example 1 a bit better. The primary decomposition of the ideal (f, g) shows that*

$$R/(f, g) \cong \mathbb{F}_2[x]/(x^3 + x^2 + 1) \oplus \mathbb{F}_2[x]/(x^5 + x^3 + 1) \cong \mathbb{F}_8 \oplus \mathbb{F}_{32}. \quad (26)$$

Multiplication by x has order 7 and 31 on each component, respectively, and order $7 \cdot 31 = 217$ on the ring $R/(f, g)$. Moreover, $y = x^{149}$ in $R/(f, g)$, so that multiplication by x and y generates the same group.

This shows that the derived automorphism T_x (or equivalently T_y) generate a cyclic group of order 217 acting by derived automorphism on K_{tile}^\bullet .

Acknowledgements — JNE was supported by Deutsche Forschungsgemeinschaft (DFG), project number 45744154, Equivariant K-motives and Koszul duality. We thank Yu-An Chen and Zijian Liang for helpful discussions.

References

- [1] S. E. Anderson, K. C. Younge, and G. Raithel. Trapping rydberg atoms in an optical lattice. *Phys. Rev. Lett.*, 107:263001, Dec 2011.
- [2] Alexandre Blais, Ren-Shou Huang, Andreas Wallraff, S. M. Girvin, and R. J. Schoelkopf. Cavity quantum electrodynamics for superconducting electrical circuits: An architecture for quantum computation. *Physical Review A*, 69(6):062320, June 2004.
- [3] S. B. Bravyi and A. Yu. Kitaev. Quantum codes on a lattice with boundary, 1998.
- [4] Sergey Bravyi, Andrew W. Cross, Jay M. Gambetta, Dmitri Maslov, Patrick Rall, and Theodore J. Yoder. High-threshold and low-overhead fault-tolerant quantum memory. *Nature*, 627(8005):778–782, March 2024.
- [5] Nikolas P. Breuckmann and Simon Burton. Fold-Transversal Clifford Gates for Quantum Codes. *Quantum*, 8:1372, June 2024.
- [6] Nikolas P. Breuckmann and Jens Niklas Eberhardt. Quantum Low-Density Parity-Check Codes. *PRX Quantum*, 2(4):040101, October 2021.

- [7] Keyang Chen, Yuanting Liu, Yiming Zhang, Zijian Liang, Yu-An Chen, Ke Liu, and Hao Song. Anyon theory and topological frustration of high-efficiency quantum low-density parity-check codes. *Phys. Rev. Lett.*, 135:076603, Aug 2025.
- [8] Alexander Cowtan and Simon Burton. Css code surgery as a universal construction. *Quantum*, 8:1344, May 2024.
- [9] Jens Niklas Eberhardt, Francisco Revson F. Pereira, and Vincent Steffan. Pruning qLDPC codes: Towards bivariate bicycle codes with open boundary conditions, 2024.
- [10] Jens Niklas Eberhardt and Vincent Steffan. Logical operators and fold-transversal gates of bivariate bicycle codes, 2024.
- [11] Austin G. Fowler, Matteo Mariantoni, John M. Martinis, and Andrew N. Cleland. Surface codes: Towards practical large-scale quantum computation. *Physical Review A*, 86(3), September 2012.
- [12] Michael H Freedman and David A Meyer. Projective plane and planar quantum codes. *Foundations of Computational Mathematics*, 1:325–332, 2001.
- [13] Markus Grassl and Martin Roetteler. Leveraging automorphisms of quantum codes for fault-tolerant quantum computation. In *2013 IEEE International Symposium on Information Theory*, page 534–538. IEEE, July 2013.
- [14] Jeongwan Haah. Commuting pauli hamiltonians as maps between free modules. *Communications in Mathematical Physics*, 324(2):351–399, Dec 2013.
- [15] D. Jaksch, J. I. Cirac, P. Zoller, S. L. Rolston, R. Côté, and M. D. Lukin. Fast quantum gates for neutral atoms. *Phys. Rev. Lett.*, 85:2208–2211, Sep 2000.
- [16] Zijian Liang, Jens Niklas Eberhardt, and Yu-An Chen. Planar quantum low-density parity-check codes with open boundaries. *PRX Quantum*, 6:040330, Nov 2025.
- [17] Zijian Liang, Ke Liu, Hao Song, and Yu-An Chen. Generalized toric codes on twisted tori for quantum error correction. *PRX Quantum*, 6:020357, Jun 2025.
- [18] Zijian Liang, Bowen Yang, Joseph T. Iosue, and Yu-An Chen. Operator algebra and algorithmic construction of boundaries and defects in (2+1)d topological pauli stabilizer codes, 2025.
- [19] Hsiang-Ku Lin and Leonid P. Pryadko. Quantum two-block group algebra codes. *Phys. Rev. A*, 109:022407, Feb 2024.
- [20] Daniel Litinski. A game of surface codes: Large-scale quantum computing with lattice surgery. *Quantum*, 3:128, March 2019.
- [21] Olivier Martin, Andrew M. Odlyzko, and Stephen Wolfram. Algebraic properties of cellular automata. *Communications in Mathematical Physics*, 93(2):219–258, 1984.
- [22] Melvin Mathews, Lukas Pahl, David Pahl, Vaishnavi L. Addala, Catherine Tang, William D. Oliver, and Jeffrey A. Grover. Placing and routing quantum ldpc codes in multilayer superconducting hardware, 2025.
- [23] Laura Pecorari, Sven Jandura, Gavin K. Brennen, and Guido Pupillo. High-rate quantum ldpc codes for long-range-connected neutral atom registers. *Nature Communications*, 16(1), January 2025.
- [24] Armando O. Quintavalle, Paul Webster, and Michael Vasmer. Partitioning qubits in hypergraph product codes to implement logical gates. *Quantum*, 7:1153, October 2023.
- [25] Michael Renger, Jeroen Verjauw, Nicola Wurz, Amin Hosseinkhani, Caspar Ockeloen-Korppi, Wei Liu, Aniket Rath, Manish J. Thapa, Florian Vigneau, Elisabeth Wybo, Ville Bergholm, Chun Fai Chan, Bálint Csatári, Saga Dahl, Rakhim Davletkaliyev, Rakshyakar Giri, Daria Gusekova, Hermanni Heimonen, Tuukka Hiltunen, Hao Hsu, Eric Hyypää, Joni Ikonen, Tyler Jones, Shabeeb Khalid, Seung-Goo Kim, Miikka Koistinen, Anton Komlev, Janne Kotilahti, Vladimir Kukushkin, Julia Lamprich, Alessandro Landra, Lan-Hsuan Lee, Tianyi Li, Per Liebermann, Sourav Majumder, Janne Mäntylä, Fabian Marxer, Arianne Meijer van de Griend, Vladimir Milchakov, Jakub Mrožek, Jayshankar Nath, Tuure Orell, Miha Papič, Matti Partanen, Alexander Plyushch, Stefan Pogorzalek, Jussi Ritvas, Pedro Figuero Romero, Ville Sampo, Marko Seppälä,

Ville Selinmaa, Linus Sundström, Ivan Takmakov, Brian Tarasinski, Jani Tuorila, Olli Tyrkkö, Alpo Välimaa, Jaap Wesdorp, Ping Yang, Liuqi Yu, Johannes Heinsoo, Antti Vepsäläinen, William Kindel, Hsiang-Sheng Ku, and Frank Deppe. A superconducting qubit-resonator quantum processor with effective all-to-all connectivity, 2025.

[26] M. Saffman, T. G. Walker, and K. Mølmer. Quantum information with rydberg atoms. *Rev. Mod. Phys.*, 82:2313–2363, Aug 2010.

[27] Chao Song, Kai Xu, Hekang Li, Yu-Ran Zhang, Xu Zhang, Wuxin Liu, Qiujiang Guo, Zhen Wang, Wenhui Ren, Jie Hao, et al. Generation of multicomponent atomic schrödinger cat states of up to 20 qubits. *Science*, 365(6453):574–577, August 2019.

[28] Chao Song, Kai Xu, Wuxin Liu, Chui-ping Yang, Shi-Biao Zheng, Hui Deng, Qiwei Xie, Keqiang Huang, Qiujiang Guo, Libo Zhang, et al. 10-qubit entanglement and parallel logic operations with a superconducting circuit. *Physical Review Letters*, 119(18), November 2017.

[29] The Stacks Project Authors. The stacks project. <https://stacks.math.columbia.edu>, 2023. Tag 015X, <https://stacks.math.columbia.edu/tag/015X>.

[30] Vincent Steffan, Shin Ho Choe, Nikolas P. Breuckmann, Francisco Revson Fernandes Pereira, and Jens Niklas Eberhardt. Tile codes: High-efficiency quantum codes on a lattice with boundary. *Phys. Rev. Lett.*, 135:170601, Oct 2025.

[31] Jean-Pierre Tillich and Gilles Zemor. Quantum ldpc codes with positive rate and minimum distance proportional to the square root of the blocklength. *IEEE Transactions on Information Theory*, 60(2):1193–1202, February 2014.

[32] Florian Vignneau, Sourav Majumder, Aniket Rath, Pedro Parrado-Rodríguez, Francisco Revson Fernandes Pereira, Hsiang-Sheng Ku, Fedor Šimkovic IV, Stefan Pogorzalek, Tyler Jones, Nicola Wurz, Michael Renger, Jeroen Verjauw, Ping Yang, William Kindel, Frank Deppe, and Johannes Heinsoo. Quantum error detection in qubit-resonator star architecture. *PRX Quantum*, pages –, Nov 2025.

[33] A. Wallraff, D. I. Schuster, A. Blais, L. Frunzio, R.-. S. Huang, J. Majer, S. Kumar, S. M. Girvin, and R. J. Schoelkopf. Strong coupling of a single photon to a superconducting qubit using circuit quantum electrodynamics. *Nature*, 431(7005):162–167, Sep 2004.

[34] Yingli Yang, Guo Zhang, and Ying Li. Planar fault-tolerant quantum computation with low overhead, 2025.

[35] Theodore J. Yoder, Eddie Schoute, Patrick Rall, Emily Pritchett, Jay M. Gambetta, Andrew W. Cross, Malcolm Carroll, and Michael E. Beverland. Tour de gross: A modular quantum computer based on bivariate bicycle codes, 2025.